

NUMERICAL SIMULATION OF THE STRUCTURE OF TIME DEPENDENT HOMOGENEOUS, ISOTROPIC TURBULENCE

by

Axel Maldonado Fernández

A thesis submitted in partial fulfillment of the requirements for the degree of

MASTER OF SCIENCE
in
MECHANICAL ENGINEERING

UNIVERSITY OF PUERTO RICO
MAYAGÜEZ CAMPUS

2007

Approved by:

Venkataraman, Nellore S, PhD
Member, Graduate Committee

Date

Gutierrez, Jorge Gustavo, PhD
Member, Graduate Committee

Date

Pandya, Raja Vikram Raj, PhD
President, Graduate Committee

Date

Paul Castillo, PhD
Representative of Graduated Studies

Date

Paul Antony Sundaram, PhD
Chairperson of the Department

Date

ABSTRACT

We consider physical situation of homogeneous, isotropic decaying turbulence in an incompressible fluid for computational study. It is well established that laminar and turbulent flows of Newtonian fluids are governed by Navier-Stokes equations. We use Navier-Stokes equations for simulating the physical situation. As no external forcing is present in the present situation, turbulence decays in time from its initial conditions. The time dependent Navier-Stokes equations are numerically solved in the Fourier wave vector (\mathbf{k}) and time (t) domain using different initial conditions for velocity field in the wave vector domain. The initial conditions are generated using the initial known shape for energy spectrum. Time evolutions of various statistical properties of isotropic turbulence are obtained from the numerical data and are presented in this thesis.

To my family . . .

ACKNOWLEDGEMENTS

Through the development of the master degree in the Mechanical Engineer Department, a lot of people has brought me a support to stand and to work everyday. Since there are not enough spaces to mentions all their names, I will only mention those who were closer.

I would like to start expressing a sincere acknowledgement to my advisor, Dr. R. Vikram Raj Pandya because he gave me his trust to develop this project. He also brought me the support and the tools to keep working on it. Other professors that I want to thank sincerely are Dr. Fred Just and to our director Dr. Paul Sundaram. I also thank the rest of the mechanical engineer department professors and personal employed for being patient with me since I started to study. Finally I want to say thanks from the heart to the general engineer department people whom were there and gave me the hand when I needed most. I acknowledge financial support provided to me for one semester by NASA EPSCoR.

Table of Contents

ABSTRACT.....	II
ACKNOWLEDGEMENTS.....	IV
TABLE OF CONTENTS.....	V
TABLE LIST.....	VI
FIGURE LIST.....	VII
1 INTRODUCTION.....	2
1.1 MOTIVATION.....	4
1.2 LITERATURE REVIEW.....	5
1.3 SUMMARY OF FOLLOWING CHAPTERS.....	6
2 THEORETICAL BACKGROUND.....	7
2.1 NUMERICAL SOLUTION OF NAVIER-STOKES EQUATIONS.....	7
2.1.1 <i>Introduction</i>	7
2.1.2 <i>Governing Equations and Numerical Procedure</i>	7
2.1.3 <i>Convective Terms</i>	14
2.1.4 <i>Initial Conditions</i>	14
3 DECAYING ISOTROPIC TURBULENCE: NUMERICAL SIMULATION RESULTS.....	16
3.1 INITIAL SPECTRA.....	16
3.2 A FEW STATISTICAL PROPERTIES.....	18
3.3 TIME EVOLUTION OF ENERGY SPECTRA I, II, III AND IV.....	20
3.4 TIME EVOLUTIONS OF VARIOUS INTEGRAL PROPERTIES.....	23
4 CONCLUDING REMARKS.....	33
REFERENCES.....	34
APPENDIX A.....	37
POST PROCESSING FOR OTHER VALUES OF Δt FOR SPECTRUM EVOLUTIONS.....	37

Table List

Tables	Page
TABLE 3.1 Values of constants c in $E(k,0) = c_1 k^{c_2} \exp(-c_3 k^{c_4})$	17

Figure List

Figures	Page
Figure 3.1 Energy Spectra at initial time.	17
Figure 3.2 Iso-Surface for x component of velocity with value -1.60594238997 at initial time for spectrum I.	18
Figure 3.3 Temporal evolution energy spectrum I for a Δt time step of .001 sec.	21
Figure 3.4 Energy Spectra II for a Δt step of .001	21
Figure 3.5 Energy Spectra III for a Δt step of .001	22
Figure 3.6 Energy Spectra IV for a Δt step of .001	22
Figure 3.7 Temporal evolution of kinetic energy per unit mass for initial energy spectra I, II, III and IV.	24
Figure 3.8 Temporal evolution of r.m.s. velocity component for initial spectra I, II, III and IV.	24
Figure 3.9 Temporal evolution of rate of dissipation of energy for spectrum I, II, III and IV.	25
Figure 3.10 Temporal evolution of integral length scale for spectrum I, II, III and IV.	26
Figure 3.11 Temporal evolution of Taylor microscale $\lambda(t)$ for spectrum I, II, III and IV.	26
Figure 3.12 Temporal evolution of Reynolds number for spectrum I.	27
Figure 3.13 Temporal evolution of Reynolds number for spectrum II.	27
Figure 3.14 Temporal evolution of Reynolds number for spectrum III.	28
Figure 3.15 Temporal evolution of Reynolds number for spectrum IV.	28
Figure 3.16 Temporal evolution of Kraichnan's characteristic wavenumber.	29
Figure 3.17 Temporal evolution of Kraichnan's characteristic velocity.	29
Figure 3.18 Temporal evolution of Kolmogorov time scale spectrum I, II, III and IV.	30
Figure 3.19 Temporal evolution of Kolmogorov length scale spectrum I, II, III and IV.	30
Figure 3.20 Evolution of dimensionless kinetic energy and dissipation vs. dimensionless time for spectrum I.	31
Figure 3.21 Evolution of dimensionless kinetic energy and dissipation vs. dimensionless time for spectrum II.	31
Figure 3.22 Evolution of dimensionless kinetic energy and dissipation vs. dimensionless time for spectrum III.	32
Figure 3.23 Evolution of dimensionless kinetic energy and dissipation vs. dimensionless time for spectrum IV.	32

1 INTRODUCTION

Turbulent flows are frequent in nature and in flow situations of many engineering equipments. These flows are unsteady, irregular and random in nature and contain circulation of fluids (eddies) of different sizes. For many years, understanding and prediction of turbulent flows have remained central goals for physicists and engineers. Though many advances have been achieved in the field, turbulence continues to surprise and defeat us in completely understanding and predicting it. This has largely due to complexity of the turbulent flows which involve interaction of large number of eddies of different sizes and eddy turnover time scales. Generating detailed information about time dependent behavior of these eddies in general situations require accurate initial and boundary conditions which are extremely difficult, if not possible, to obtain. Further implementation of these in numerical methods and simulating the turbulent flows in general by using Navier-Stokes equations require computer resources and computing speed which are not yet available. At present, it is possible to simulate turbulent flows in simple geometries and not at very large Reynolds numbers.

For this work, we consider simulation of ideal situation of homogeneous, isotropic turbulence in an incompressible fluid. This situation is studied numerically by many researchers and continues to remain as an active field of research. The numerical study on this situation provides data for testing various theories generated for turbulence and the data also reveal fundamental properties and phenomena of turbulence.

The homogeneity of the turbulent flow field means that the statistical properties of turbulence are independent of location of coordinate system in which these properties are obtained. Further, if the statistical properties are independent of rotation and mirror image of the coordinate system, turbulence is called isotropic. So homogeneous isotropic turbulence does not have any preference for the direction of the flow and statistical mean velocity and mean pressure gradient field is zero. In the absence of any imposed external forcing, this situation contains only interaction of different eddies of different sizes and time scales. The fluid viscosity (friction between fluid layers) causes slowing down of these fluid circulations (eddies) in time. And finally the fluid turbulence will come to rest. All the kinetic energy (due to non zero velocity field) which the flow had at some initial time is converted ultimately into heat due to the presence of viscosity.

This situation of homogeneous, isotropic turbulence is studied here by performing direct numerical simulation (DNS) of Navier-Stokes equations. We consider incompressible Newtonian fluid in a domain $2\pi \times 2\pi \times 2\pi \text{ m}^3$. The Reynolds number and consequently the range for size of interacting eddies are considered sufficiently small so that the simulation can be performed on laptop on the grid size $64 \times 64 \times 64$. In case of isotropic turbulence, periodic boundary conditions are employed as there is no preferred direction for the mean flow. Navier-Stokes equations are solved in discrete Fourier wave vector and time domain. The initial conditions for isotropic turbulence are generated by using different shapes of energy spectrum. The details of initial conditions are described later in Chapters 2 and 3. The energy spectrum indicates how the kinetic energy of turbulence is distributed among various

Fourier modes (\mathbf{k}) which roughly indicates inverse of size of eddies. This means that large eddy has small value for $k = |\mathbf{k}|$ representing magnitude of \mathbf{k} and smaller eddy has large value for k .

1.1 Motivation

In environmental and engineering situations having large length scales, turbulent flows occur as a rule rather than exception. All kinds of turbulent flows at large Reynolds number have universal scaling, known as Kolmogorov scaling, behavior in certain range of length scales near smaller eddy sizes. Also, in this range turbulence is locally isotropic as suggested by Kolmogorov. To understand the universal behavior of locally isotropic nature of turbulent flows, it becomes necessary to analyze ideal situation of homogeneous, isotropic turbulence. This ideal situation is though accessible for theoretical analysis, it is most difficult if not impossible to generate experimentally. To assess the theoretical developments and predictions of homogeneous isotropic turbulence, computational simulation of such an ideal flow becomes necessary. In view of these, the present study is undertaken to generate temporal behavior of statistical properties of homogeneous, isotropic turbulence through direct numerical simulation. The information on time dependent statistical properties can be used to assess predictions of various theories of statistical turbulence which have been proposed by researchers (see McComb 1990 and references cited therein).

1.2 Literature Review

The first numerical study on decaying homogeneous, isotropic turbulence was performed by Orszag and Patterson (1972). They solved the three-dimensional Navier-Stokes equations for incompressible flow numerically in Fourier wave vector and time domain. Using their numerical simulation data, they performed assessment of a theory of statistical turbulence proposed by Kraichnan (1959). Their numerical study was performed for the Taylor microscale based Reynolds number values less than 45. After this study, there have been increased activities for simulating ideal situation of isotropic turbulence and utilizing it for assessing various statistical theories of turbulence (McComb 1992) and generating fundamental understanding of turbulence. For example, McComb and his coworkers (see references McComb and Shanmugasundaram 1984, McComb and Quinn 2003, Kuczaj, Geurts and McComb 2006 and references cited therein) have performed numerical simulation of decaying and stationary isotropic turbulence to understand interactions between various wave vectors (eddies) and to assess their theory which is well known as Local Energy Transfer (LET) theory.

Isotropic turbulence simulations have also been performed by Yueng and his coworkers to study statistical properties of passive scalar field such as temperature (Donzis, Sreenivasan, Yueng 2005) and Lagrangian statistics of velocity and scalar fields (Yueng 2001).

Numerical simulation of isotropic turbulence is also utilized by researchers working in the field of multiphase turbulent flows (see review by Mashayek and Pandya 2003). The cases of

isotropic turbulence seeded with a large number of particles/droplets/bubbles provide extremely rich database and statistical properties of velocity, temperature, dispersion, collision behavior of these particles/droplets/bubbles. These kind of studies provide insight into multiphase flows relevant to many important situations of technology and environmental flows, such as, spray combustion and collision statistics of droplets for modeling of cloud microphysics (Sundaram and Collins 1997).

Though the above mentioned literature do not cover all aspects of fundamental studies on isotropic turbulence, it exhibit important application areas of isotropic turbulence simulations. In view of above mentioned usefulness of isotropic turbulence, in this thesis we undertake numerical simulation studies of decaying isotropic turbulence. The results presented here will be used later to assess a theory of turbulence (Pandya 2004), known as Variant of Local Energy Transfer theory.

1.3 Summary of Following Chapters

We first develop the necessary background theory in Chapter 1. Chapter 2 deals with the numerical methodology for decaying isotropic turbulence and generation of initial conditions for simulations. The third chapter presents temporal variations of various statistical properties of isotropic turbulence as obtained through numerical simulations for cases having different initial conditions. Concluding remarks are presented in Chapter 4.

2 THEORETICAL BACKGROUND

2.1 Numerical Solution of Navier-Stokes Equations

2.1.1 Introduction

It is well established that laminar, transition and turbulent regimes of Newtonian fluid flows are governed by the Navier-Stokes equations which consist of conservation of mass and momentum equations. We will use Navier-Stokes equations and numerically compute these equations in Fourier wave vector and time domain. The methodology adopted here is well established for accurate computation of homogeneous, isotropic turbulence. Periodic boundary conditions will be used along with the initial conditions generated from the known shape of the energy spectrum. The details of the methodology and initial conditions are presented in this chapter.

2.1.2 Governing Equations and Numerical Procedure

The Navier-Stokes equations governing the incompressible fluid flow situation can be written as,

Momentum Equation:

$$\frac{\partial \underline{u}}{\partial t} + u \frac{\partial \underline{u}}{\partial x} + v \frac{\partial \underline{u}}{\partial y} + w \frac{\partial \underline{u}}{\partial z} = -\frac{1}{\rho} \vec{\nabla}(p) + \nu \left(\frac{\partial^2 \underline{u}}{\partial x^2} + \frac{\partial^2 \underline{u}}{\partial y^2} + \frac{\partial^2 \underline{u}}{\partial z^2} \right) \quad 2.1$$

Continuity Equation:

$$\frac{\partial u}{\partial x} + \frac{\partial v}{\partial y} + \frac{\partial w}{\partial z} = 0,$$

where $\underline{u} = \{u, v, w\}$ is velocity vector field with velocity components $\{u, v, w\}$ along the $\{x, y, z\}$ directions, respectively, p is the pressure, ρ is density of fluid and ν is the kinematic viscosity. For the convenience of discussion, nonlinear term (convective term) appearing in the momentum equation is represented by \underline{f} so that the equation (2.1) can be written as

$$\frac{\partial \underline{u}}{\partial t} + \underline{f} = -\frac{1}{\rho} \vec{\nabla}(p) + \nu \left(\frac{\partial^2 \underline{u}}{\partial x^2} + \frac{\partial^2 \underline{u}}{\partial y^2} + \frac{\partial^2 \underline{u}}{\partial z^2} \right), \quad 2.2$$

where

$$\underline{f} \equiv u \frac{\partial \underline{u}}{\partial x} + v \frac{\partial \underline{u}}{\partial y} + w \frac{\partial \underline{u}}{\partial z}. \quad 2.3$$

For homogeneous, isotropic turbulence case, these governing equations are solved in a domain of $2\pi \times 2\pi \times 2\pi \text{ m}^3$ by utilizing spectral method similar to that provided by Rogallo (1981) and is also described by Copen (1998). The Reynolds number is considered sufficiently small so that the simulation can be performed on laptop on the grid size $64 \times 64 \times 64$. In case of isotropic turbulence, periodic boundary conditions are employed as

there is no preferred direction for the mean flow. Now we discuss spectral method used for numerical simulation.

Equation (2.2) which is written in physical space is transformed into Fourier wave vector domain. To do this, we now discuss three dimensional discrete Fourier series for velocity vector field and pressure.

The discrete three dimensional Fourier transform of a fluid velocity and pressure can be written as

$$\tilde{\underline{u}}(\underline{\kappa}_n, t) = \frac{1}{N^3} \sum_{x_m=0}^{N-1} \sum_{y_m=0}^{N-1} \sum_{z_m=0}^{N-1} \underline{u}(\underline{x}_m, t) e^{-i(k_{x_n} x_m + k_{y_n} y_m + k_{z_n} z_m)}, \quad 2.4$$

$$\tilde{p}(\underline{\kappa}_n, t) = \frac{1}{N^3} \sum_{x_m=0}^{N-1} \sum_{y_m=0}^{N-1} \sum_{z_m=0}^{N-1} p(\underline{x}_m, t) e^{-i(k_{x_n} x_m + k_{y_n} y_m + k_{z_n} z_m)}, \quad 2.5$$

where $\tilde{\underline{u}}$ and \tilde{p} represent discrete Fourier transformed of fluid velocity vector and pressure, respectively when u and p are known at discrete grid points \underline{x}_n in physical domain. While writing equations (2.4) and (2.5), length of the domain along all three directions is considered equal and identical to 2π . The parameter $\underline{\kappa}_n$ represents Fourier wave vector having components $k_{x_n}, k_{y_n}, k_{z_n}$. These components are given as

$$\underline{\kappa}_n = (k_{x_n}, k_{y_n}, k_{z_n}) \equiv \begin{cases} \left(\frac{2\pi n}{N\delta}, \frac{2\pi n}{N\delta}, \frac{2\pi n}{N\delta} \right); n < \frac{N}{2} \\ \left(\frac{2\pi(N-n)}{N\delta}, \frac{2\pi(N-n)}{N\delta}, \frac{2\pi(N-n)}{N\delta} \right); n \geq \frac{N}{2} \end{cases} \quad 2.6$$

where δ represents spacing between two grid points along any direction and is considered identical along all three directions. The discrete three-dimensional inverse Fourier transformation for equations (2.4) and (2.5) can be written as

$$\underline{u}(\underline{x}_n, t) = \sum_{\kappa_{x_m}=0}^{N-1} \sum_{\kappa_{y_m}=0}^{N-1} \sum_{\kappa_{z_m}=0}^{N-1} \tilde{u}(\underline{\kappa}_m, t) e^{+i(k_{x_m} x_n + k_{y_m} y_n + k_{z_m} z_n)}, \quad 2.7$$

$$p(\underline{x}_n, t) = \sum_{\kappa_{x_m}=0}^{N-1} \sum_{\kappa_{y_m}=0}^{N-1} \sum_{\kappa_{z_m}=0}^{N-1} \tilde{p}(\underline{\kappa}_m, t) e^{+i(k_{x_m} x_n + k_{y_m} y_n + k_{z_m} z_n)}, \quad 2.8$$

The spatial derivative of the fluid velocity and pressure can be obtained from equations (2.7) and (2.8). From the definition of Fourier transform and inverse Fourier transform, it can be

shown that Fourier transform of $\frac{\partial \underline{u}}{\partial x}$ and $\left(\frac{\partial^2 \underline{u}}{\partial x^2} + \frac{\partial^2 \underline{u}}{\partial y^2} + \frac{\partial^2 \underline{u}}{\partial z^2} \right)$ are

$$ik_x \tilde{\underline{u}} \quad \text{and} \quad -(k_x^2 + k_y^2 + k_z^2) \tilde{\underline{u}}. \quad 2.9$$

Using all these we can now write Navier-Stokes equation (2.2) in the Fourier domain as

$$\frac{\partial}{\partial t} \tilde{u} + \tilde{f} = -\frac{1}{\rho} i k \tilde{p} - \nu (k_x^2 \tilde{u} + k_y^2 \tilde{u} + k_z^2 \tilde{u}), \quad 2.10$$

where \tilde{f} represent Fourier transform of convective term and detail for its calculations are provided later in this chapter.

To calculate pressure \tilde{p} , we can utilize continuity equation. The Fourier transform of continuity equation can be written as

$$\text{Continuity equation: } \frac{\partial u}{\partial x} + \frac{\partial v}{\partial y} + \frac{\partial w}{\partial z} = 0 \quad \text{Fourier transform: } k_x \tilde{u} + k_y \tilde{v} + k_z \tilde{w} = 0. \quad 2.11$$

Now we obtain divergence of (2.10) in Fourier domain. Multiplying three equations, obtained from vector equation (2.10), for components \tilde{u} , \tilde{v} , and \tilde{w} by k_x , k_y and k_z , respectively, we obtain

$$xdir: \frac{\partial}{\partial t} k_x \tilde{u} + \nu (k_x^2 + k_y^2 + k_z^2) k_x \tilde{u} + k_x \tilde{f}_x = -\frac{1}{\rho} i k_x^2 \tilde{p}, \quad 2.12$$

$$ydir: \frac{\partial}{\partial t} k_y \tilde{v} + \nu (k_x^2 + k_y^2 + k_z^2) k_y \tilde{v} + k_y \tilde{f}_y = -\frac{1}{\rho} i k_y^2 \tilde{p}, \quad 2.13$$

$$zdir: \frac{\partial}{\partial t} k_z \tilde{w} + \nu(k_x^2 + k_y^2 + k_z^2) k_z \tilde{w} + k_z \tilde{f}_z = -\frac{1}{\rho} i k_z^2 \tilde{p}. \quad 2.14$$

By adding (2.12), (2.13), and (2.14) and utilizing (2.11), we obtain

$$k_x \tilde{f}_x + k_y \tilde{f}_y + k_z \tilde{f}_z = -\frac{1}{\rho} i (k_x^2 + k_y^2 + k_z^2) \tilde{p} \quad 2.15$$

and from which \tilde{p} can be obtained if components of Fourier transform of convective term i.e.

$\tilde{f}_x, \tilde{f}_y, \tilde{f}_z$ are known. Using equation (2.15), equation (2.10) can be written after eliminating

pressure term as

$$\frac{\partial}{\partial t} \tilde{u} + \nu(k_x^2 + k_y^2 + k_z^2) \tilde{u} = \kappa \left(\frac{k_x \tilde{f}_x + k_y \tilde{f}_y + k_z \tilde{f}_z}{k_x^2 + k_y^2 + k_z^2} \right) - \tilde{f}. \quad 2.16$$

This equation (2.16) can be further written in simplified form by using an integrating factor

$h(t)$ whereby the viscous terms is treated exactly. Then (2.16) can be modified to the form

$$\frac{\partial}{\partial t} (\tilde{u} h(t)) = \left[\kappa \left(\frac{k_x \tilde{f}_x + k_y \tilde{f}_y + k_z \tilde{f}_z}{k_x^2 + k_y^2 + k_z^2} \right) - \tilde{f} \right] h(t), \quad 2.17$$

where

$$h(t) = \exp\left(\nu(k_x^2 + k_y^2 + k_z^2)t\right) \quad 2.18$$

This equation (2.17) represents initial value problem with prescribed initial conditions for \tilde{u} and can be solved with suitable numerical scheme(s), such as forward Euler method, Runge-Kutta method of order three or higher.

For example, if we consider Euler method as utilized by Coppen (1998) for isotropic turbulence simulations, equation (2.17) can be discretized as

$$\frac{\tilde{u}^{n+1}h(t + \delta t) - \tilde{u}^n h(t)}{\delta t} \cong RHS(2.16)h(t), \quad 2.19$$

where δt represents time step. As $h(t)$ is an exponential function in time

$$h(t + \delta t) = \exp\left[\nu(k_x^2 + k_y^2 + k_z^2)(t + \delta t)\right] = h(t)h(\delta t). \quad 2.20$$

Substituting (2.20) into (2.19) and after simplification we obtain

$$\tilde{u}^{n+1} \cong \frac{\tilde{u}^n + RHS(2.16)\delta t}{h(\delta t)} \quad 2.21$$

which can be used to solve numerically time evolution of Fourier modes $\underline{\tilde{u}}$ of isotropic velocity field.

2.1.3 Convective Terms

In order to solve numerically equation (2.16), we need information about Fourier transform of convective term, i.e. $\underline{\tilde{f}}$, at each time step. Now we discuss the calculation procedure for this term.

First at each time step, velocity field in physical space \underline{u} and its spatial derivatives are obtained by inverse transform of the velocity field in the Fourier domain $\underline{\tilde{u}}$ and $(ik_x \underline{\tilde{u}}, ik_y \underline{\tilde{u}}, ik_z \underline{\tilde{u}})$, respectively. From the obtained velocity field and its spatial derivatives, convective terms \underline{f} as given by equation (2.3) are calculated in physical domain. These calculated terms \underline{f} are then transformed into Fourier wave vector domain.

2.1.4 Initial Conditions

In order to solve discretized form of equation (2.16), such as equation (2.21), we need initial values at time $t = 0$ for $\underline{\tilde{u}}(\underline{\kappa}, t = 0) = \underline{\tilde{u}}(\underline{\kappa})$ at all grid points $\underline{\kappa}_n$ of Fourier domain. The initial values are calculated in such a manner that the velocity field is compatible with certain energy spectrum shape $E(k)$ at time $t = 0$. We use the method of Rogallo (1981) for this purpose which suggests final formula for generating $\underline{\tilde{u}}(\underline{\kappa})$ as

$$\tilde{u}(\underline{\kappa}) = \left(\frac{\alpha k k_2 + \beta k_1 k_3}{k(k_1^2 + k_2^2)^{1/2}} \right) \underline{e}_1 + \left(\frac{\beta k_3 k_2 - \alpha k k_1}{k(k_1^2 + k_2^2)^{1/2}} \right) \underline{e}_2 - \left(\frac{\beta(k_1^2 + k_2^2)^{1/2}}{k} \right) \underline{e}_3 \quad 2.22$$

Here α and β are given by

$$\alpha = \left(\frac{E(k)}{4\pi k^2} \right)^{1/2} \exp(i\theta_1) \cos \phi \quad 2.23$$

$$\beta = \left(\frac{E(k)}{4\pi k^2} \right)^{1/2} \exp(i\theta_2) \sin \phi \quad 2.24$$

In the above equations, θ_1, θ_2 and ϕ are random numbers statistically independent of each other and uniformly distributed in the range 0 to 2π .

3 DECAYING ISOTROPIC TURBULENCE: NUMERICAL SIMULATION RESULTS

Various direct numerical simulation cases were carried out for different initial conditions for velocity field in the Fourier space consistent with the selected initial spectra. The results of these simulations are presented here after presenting the information for initial spectra and statistical properties considered for temporal evolution for homogeneous isotropic turbulence.

3.1 Initial Spectra

Four different initial energy spectra $E(k,t=0)$ were used to calculate initial conditions for velocity field. The general form of these energy spectra is given by

$$E(k,0) = c_1 k^{c_2} \exp(-c_3 k^{c_4}), \quad 3.1$$

where c_1, c_2, c_3 and c_4 are constants. The details of these constants for different spectra are provided in TABLE . Also these spectra are plotted in Fig. 3.1. These spectra are identical to the spectra considered by McComb and Shanmugasundaram (1984) for low Reynolds number isotropic turbulence. The use of these spectra allow us to simulate isotropic turbulence on a laptop with 2GB of RAM. The grid size used for all simulations in this work

is 64x64x64 and is suitable for capturing all wave numbers of different spectra during their time evolution. Further, a typical plot of isosurface of one component of velocity that was generated by using energy spectrum I is shown in Figure 3.2.

TABLE 3.1 Values of constants c in $E(k,0) = c_1 k^{c_2} \exp(-c_3 k^{c_4})$

Spectrum Number	c_1	c_2	c_3	c_4	V (m ² /s)
I	0.524169 x 10 ⁻²	4	0.883882 x 10 ⁻¹	2	0.01189
II	0.662912 x 10 ⁻¹	1	0.220971 x 10 ⁻¹	2	0.01189
III	0.662912 x 10 ⁻¹	1	0.210224	1	0.01189
IV	0.4	1	0.5	1	0.01189

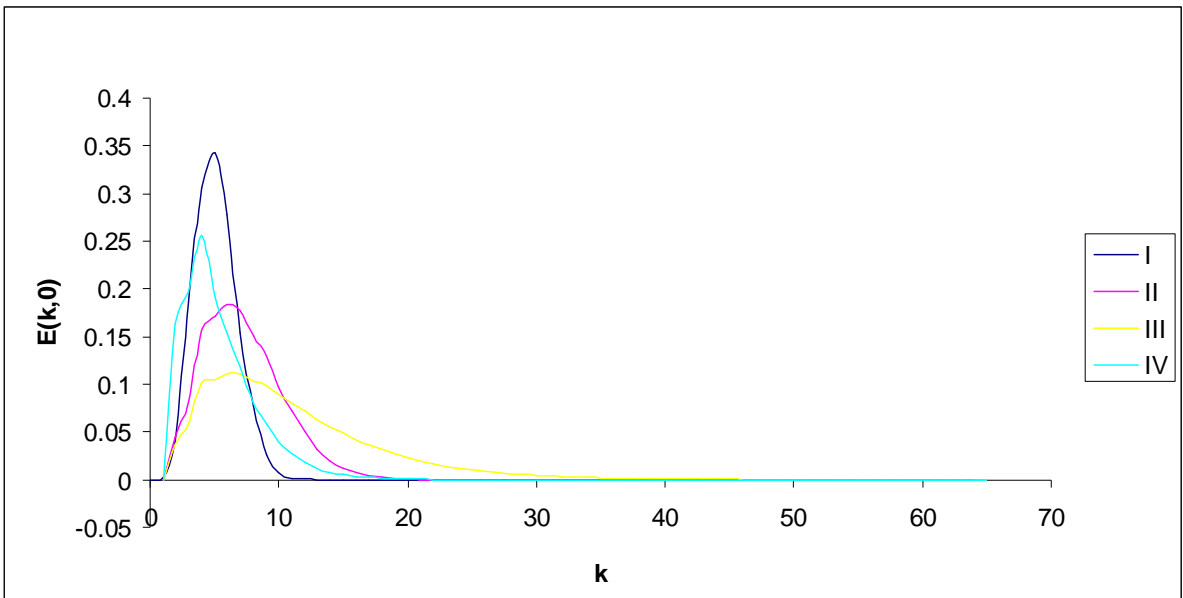


Figure 3.1 Energy Spectra at initial time.

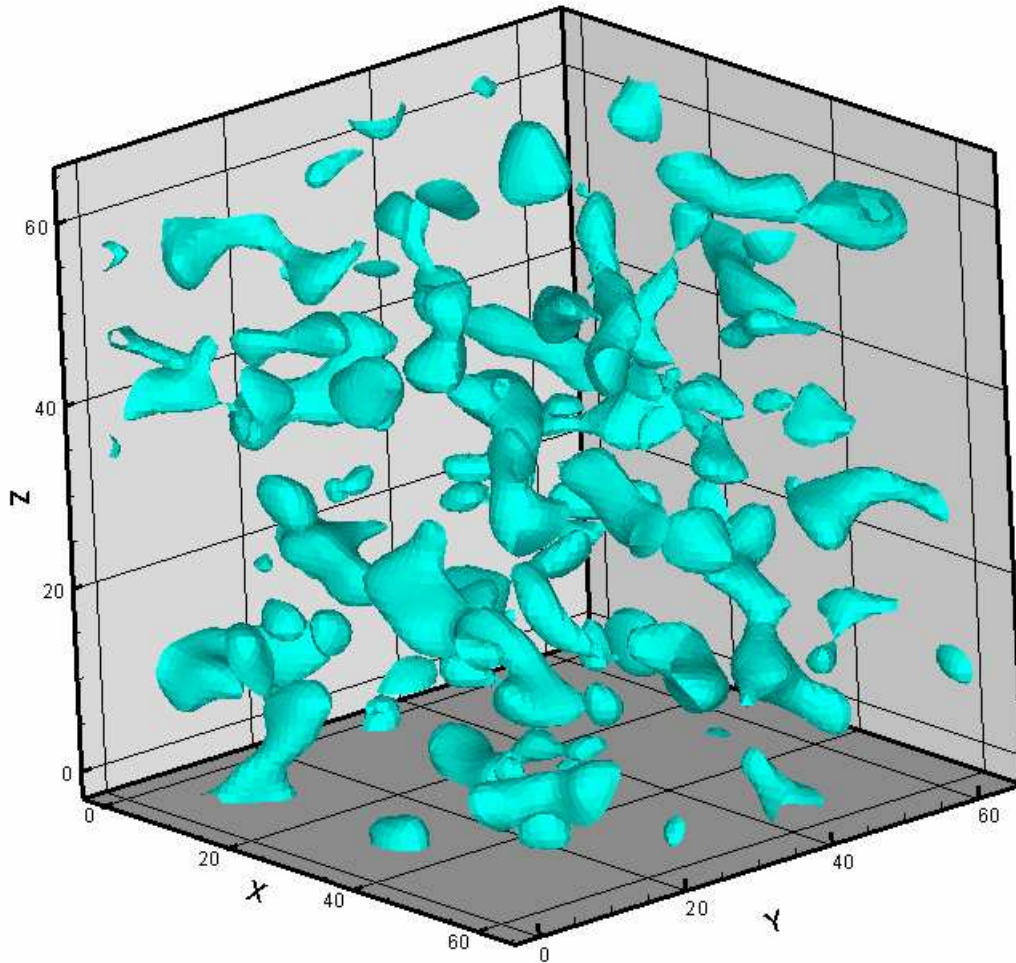


Figure 3.2 Iso-Surface for x component of velocity with value -1.60594238997 at initial time for spectrum I.

3.2 A Few Statistical Properties

Once the energy spectrum is known at each time step, different statistical properties which depend on the spectrum can be calculated from it. From the energy spectrum, we can obtain integral properties, such as, mean kinetic energy $E(t)$ per unit mass, the r.m.s. value of any

component of turbulent velocity field $u(t)$ and the dissipation of energy due to viscosity $\epsilon(t)$, the integral length scale $L(t)$ and the Taylor microscale $\lambda(t)$.

The r.m.s. of the velocity components, $u(t)$, and the rate of dissipation per unit mass can be calculated using

$$E(t) = \int_0^{\infty} E(k, t) dk = \frac{3}{2} [u(t)]^2 \quad 3.2$$

and

$$\epsilon(t) = 2\nu \int_0^{\infty} k^2 E(k, t) dk. \quad 3.3$$

The integral lengthscale $L(t)$ and the Taylor microscale $\lambda(t)$ can be obtained using

$$L(t) = \left[\frac{3\pi}{4} \int_0^{\infty} k^{-1} E(k, t) dk \right] / E(t), \quad 3.4$$

and

$$\lambda(t) = \left[5E(t) / \int_0^{\infty} k^2 E(k, t) dk \right]^{1/2}. \quad 3.5$$

The Reynolds numbers associated with these length scales are given as

$$R_L(t) = L(t) \frac{u(t)}{\nu}, \quad 3.6$$

and

$$R_\lambda(t) = \lambda(t) \frac{u(t)}{\nu}. \quad 3.7$$

Also calculated are the characteristic wavenumber and velocity scales for turbulence as suggested by Kraichnan (1964) . These are given by

$$k_d = (15R_\lambda)^{\frac{1}{3}} \lambda^{-1} \quad 3.8$$

$$v_d = (R_\lambda / 15^2)^{\frac{1}{3}} u(t) \quad 3.9$$

3.3 Time Evolution of Energy Spectra I, II, III and IV

Temporal evolution of various spectra I, II, III and IV are shown in Figure 3.3, Figure 3.4, Figure 3.5, and Figure 3.6, respectively. In these figures, time is in seconds and time step used during numerical simulation is tested for converge solutions. Also, various color lines indicate value of time at which spectrum is plotted in these figures. Tests cases were run for various values for time steps and results from a few test runs used for arriving at converged solutions are provided in Appendix A. Here we will present results for time step 0.001 sec.

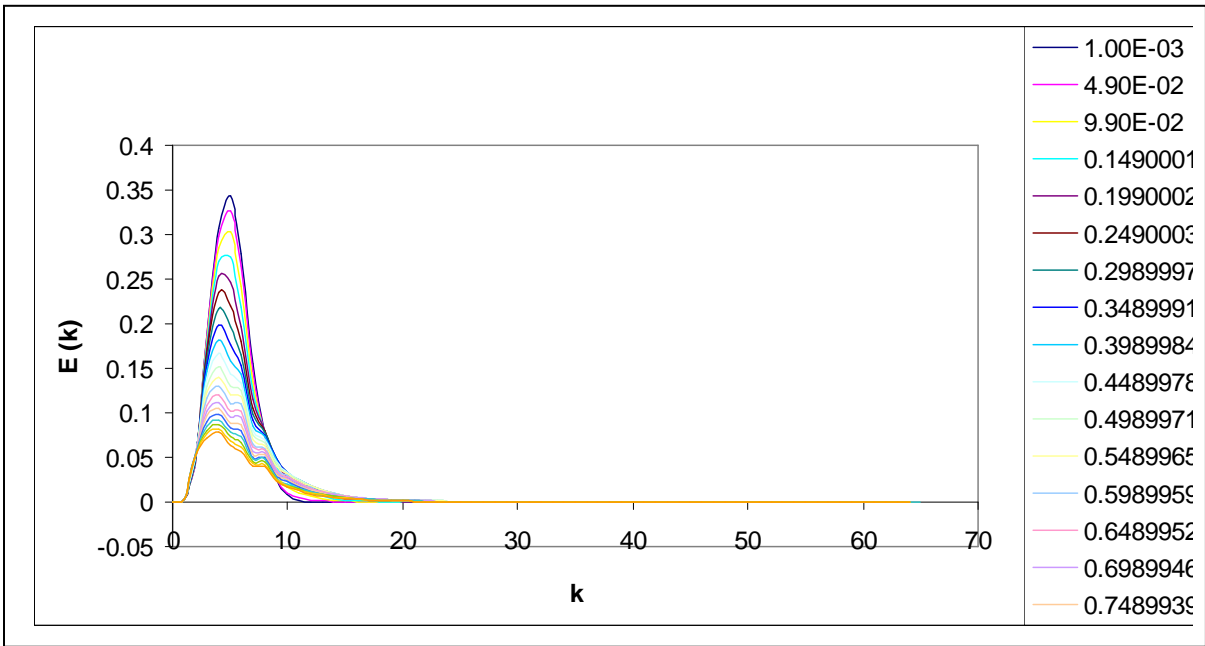


Figure 3.3 Temporal evolution energy spectrum I for a Δt time step of .001 sec.

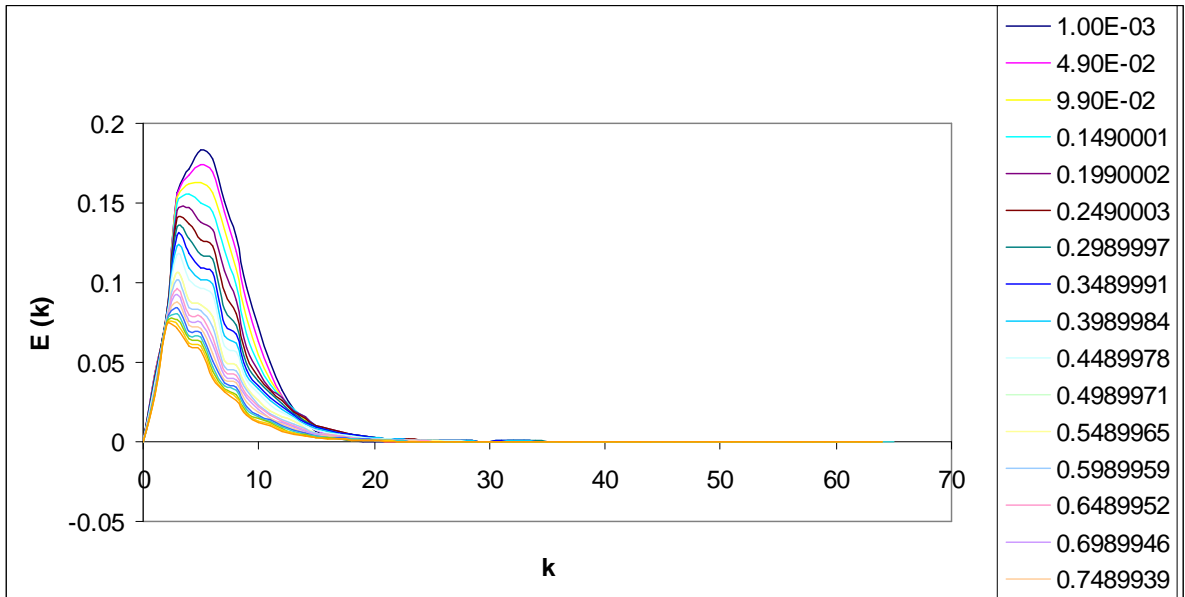


Figure 3.4 Energy Spectra II for a Δt step of .001

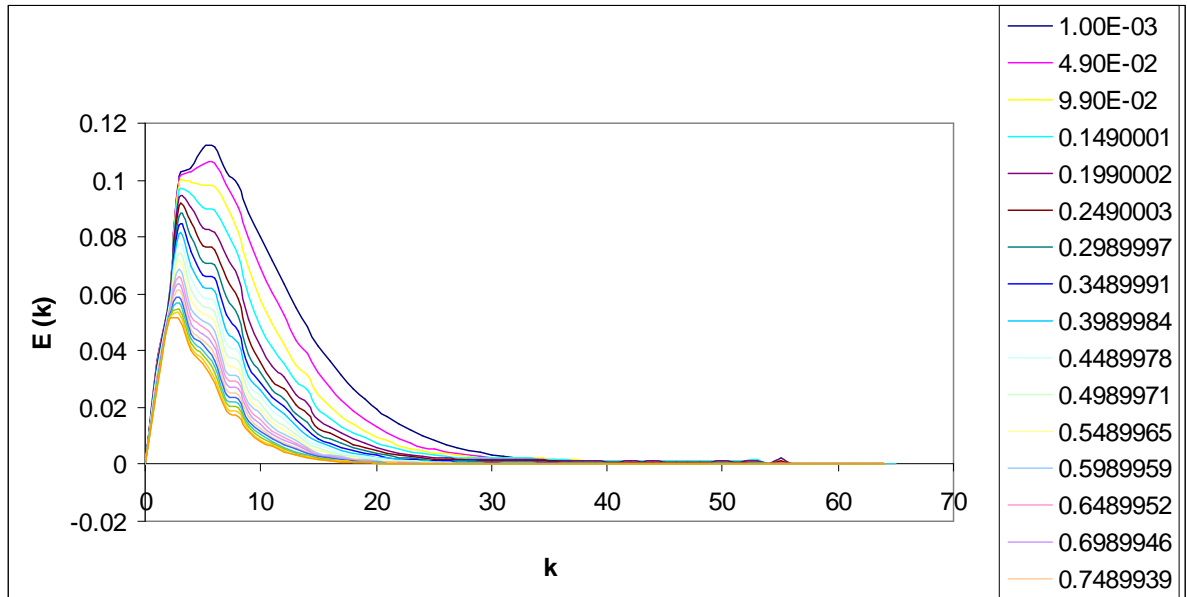


Figure 3.5 Energy Spectra III for a Δt step of .001

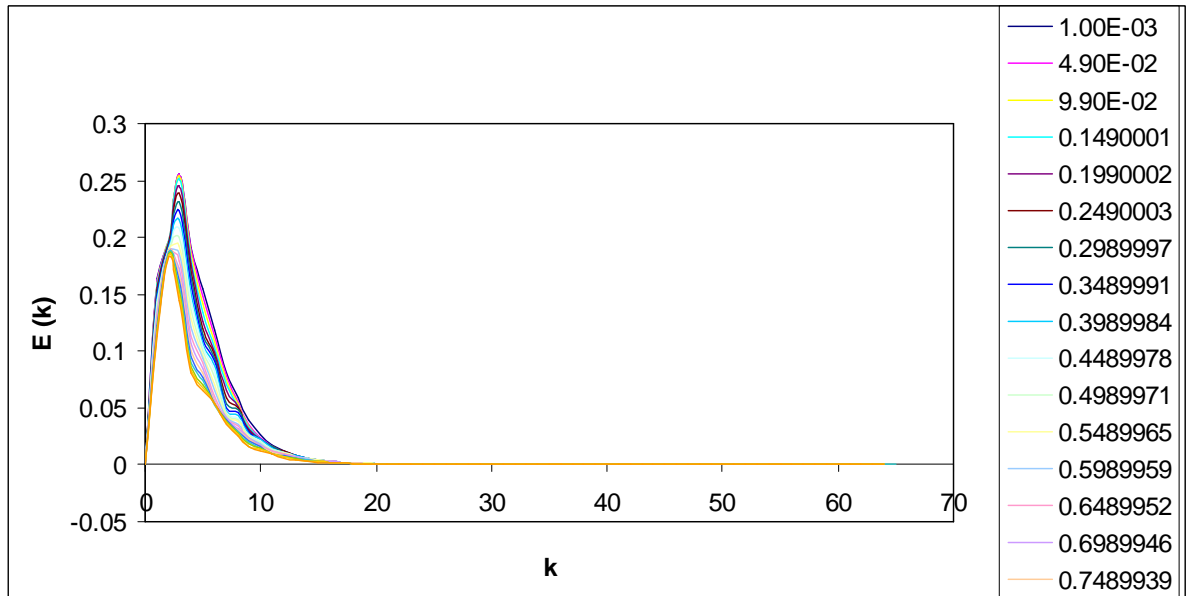


Figure 3.6 Energy Spectra IV for a Δt step of .001

3.4 Time Evolutions of Various Integral Properties

Various integral properties of isotropic turbulence can be calculated by using the energy spectrum. So by utilizing data on temporal evolution for different energy spectra I, II, III and IV, time evolutions of various integral properties are calculated. The temporal evolutions for kinetic energy per unit mass of turbulence are shown in Figure 3.1. In Figure 3.8, r.m.s. velocity component vs. time is plotted for different cases. Figure 3.9 exhibits rate of dissipation of kinetic energy of turbulence as a function of time for different initial spectra. In Figure 3.10, integral length scale (unit is meter) evolution in time is shown. This integral length scale roughly indicates the length scale of energy containing eddies. The Taylor microscale vs. time for different cases are shown in Figure 3.11. This microscale is a characteristic length scale usually used to estimate dissipation of turbulence. Integral length scale and Taylor's microscale based Reynolds numbers $R_L(t)$ and $R_\lambda(t)$ vs. time are plotted in Figure 3.12, Figure 3.13, Figure 3.14 and Figure 3.15 for cases with initial energy spectrum I, II, III and IV, respectively. Temporal evolutions for characteristic wave number and velocity scales suggested by Kraichnan are shown in Figure 3.16 and Figure 3.17, respectively. Temporal evolution of Kolmogorov time and length scales are shown in Figure 3.18 and Figure 3.19, respectively. These scales are characteristic scales of small eddies which are responsible for dissipation of turbulence kinetic energy and are in the range of smallest scales of turbulence. Further, nondimensional form of kinetic energy and dissipation of turbulence are plotted against nondimensional time in Figure 3.20, Figure 3.21, Figure 3.22, Figure 3.23 for different initial spectrum cases I, II, III and IV, respectively.

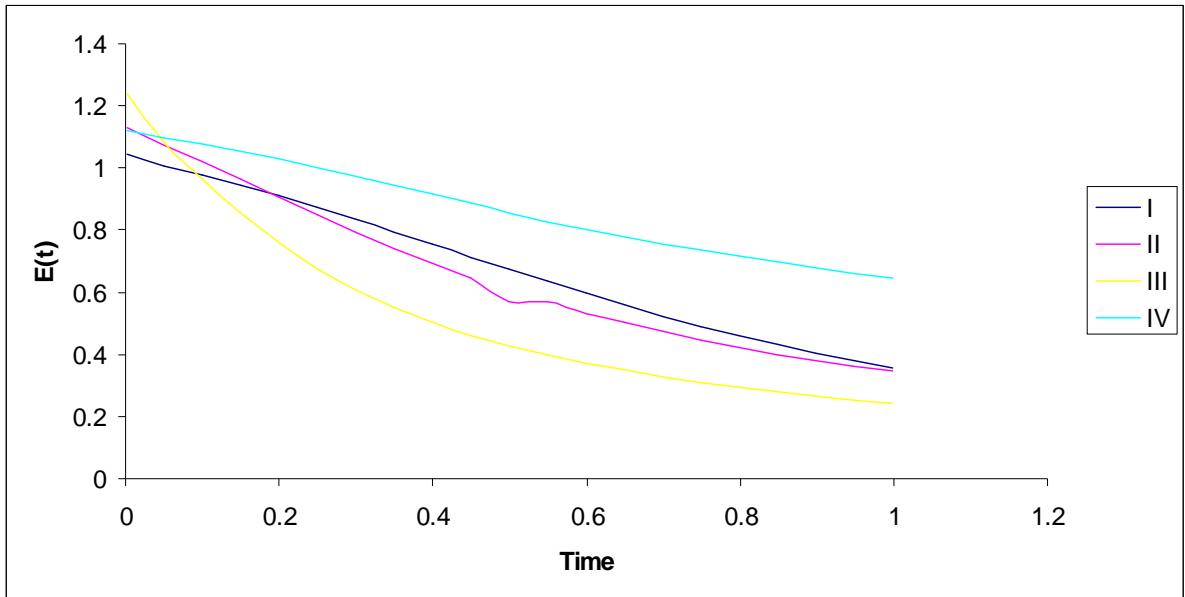


Figure 3.7 Temporal evolution of kinetic energy per unit mass for initial energy spectra I, II, III and IV

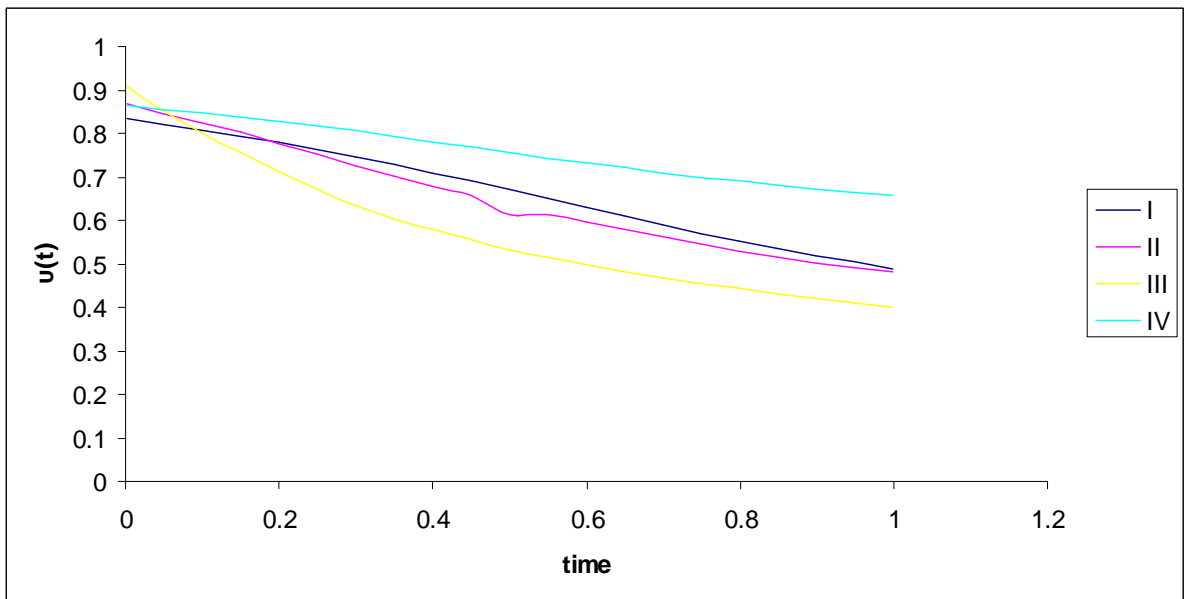


Figure 3.8 Temporal evolution of r.m.s. velocity component for initial spectra I, II, III and IV.

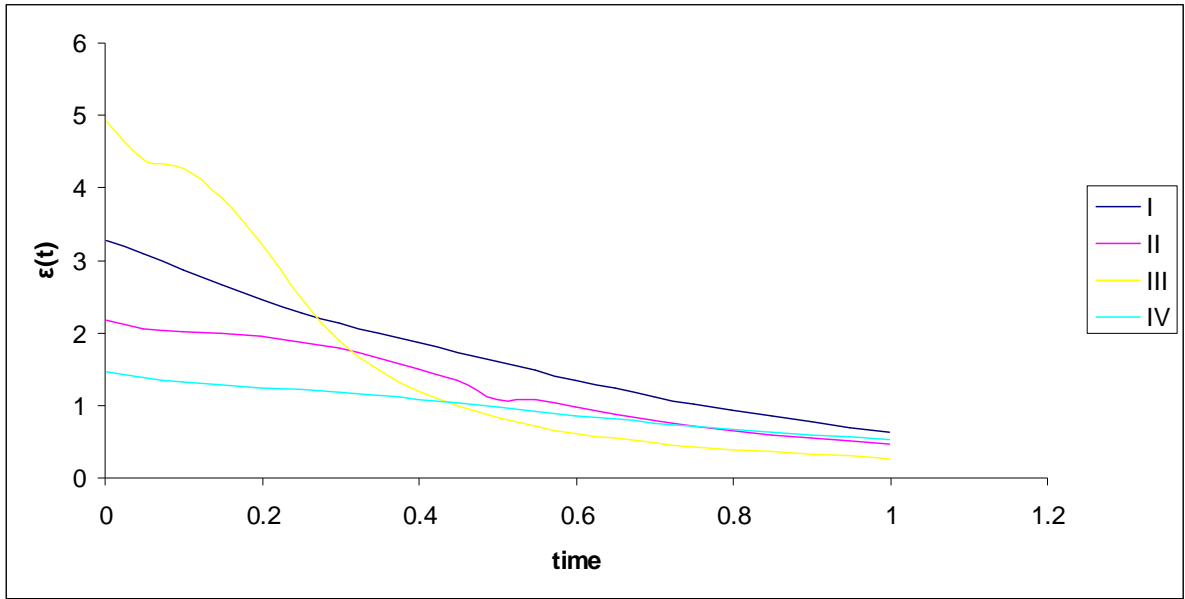


Figure 3.9 Temporal evolution of rate of dissipation of energy for spectrum I, II, III and IV.

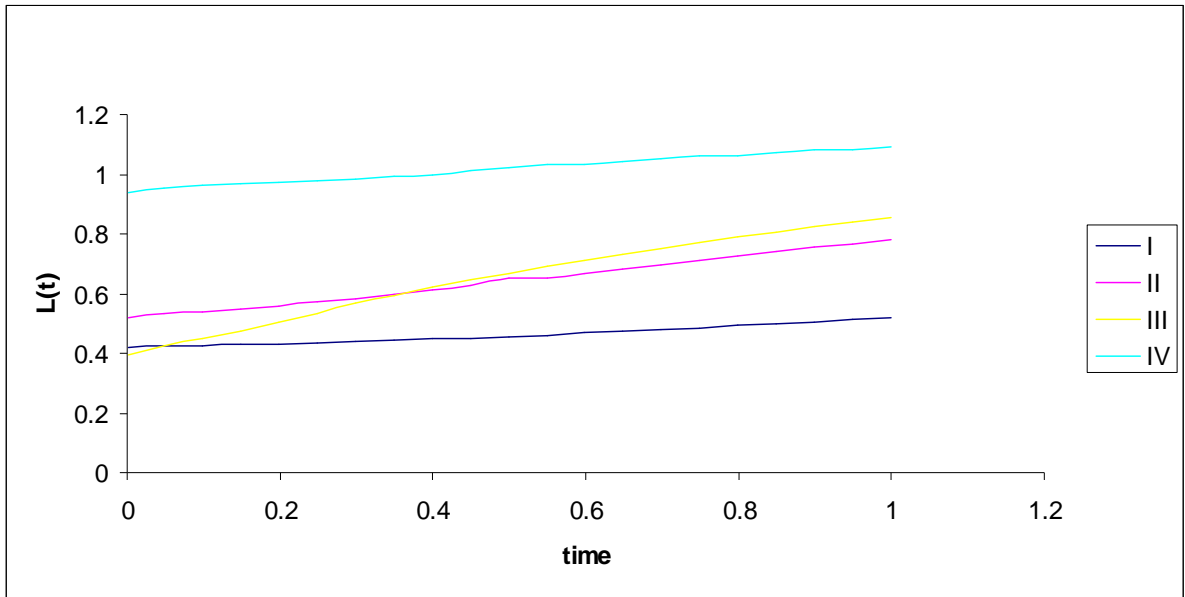


Figure 3.10 Temporal evolution of integral length scale for spectrum I, II, III and IV.

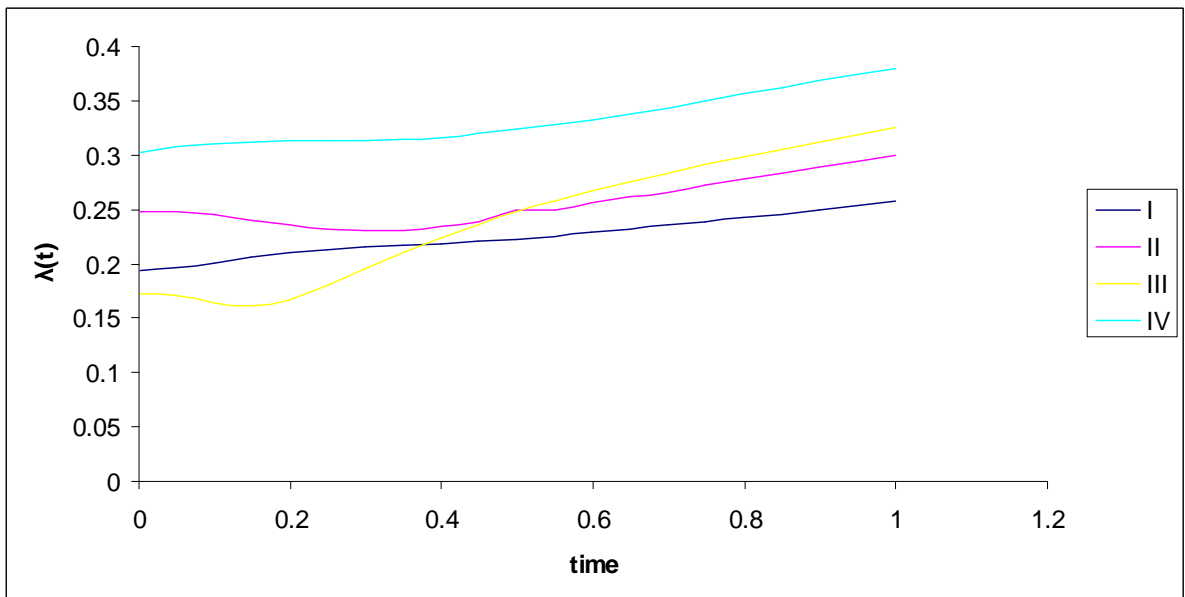


Figure 3.11 Temporal evolution of Taylor microscale $\lambda(t)$ for spectrum I, II, III and IV.

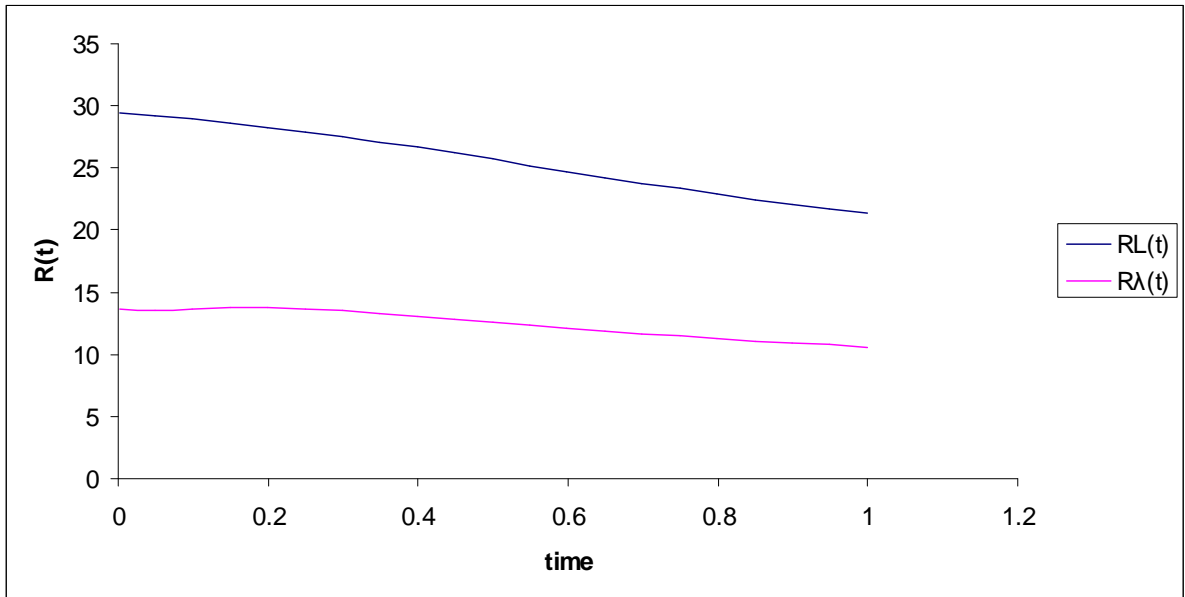


Figure 3.12 Temporal evolution of Reynolds number for spectrum I.

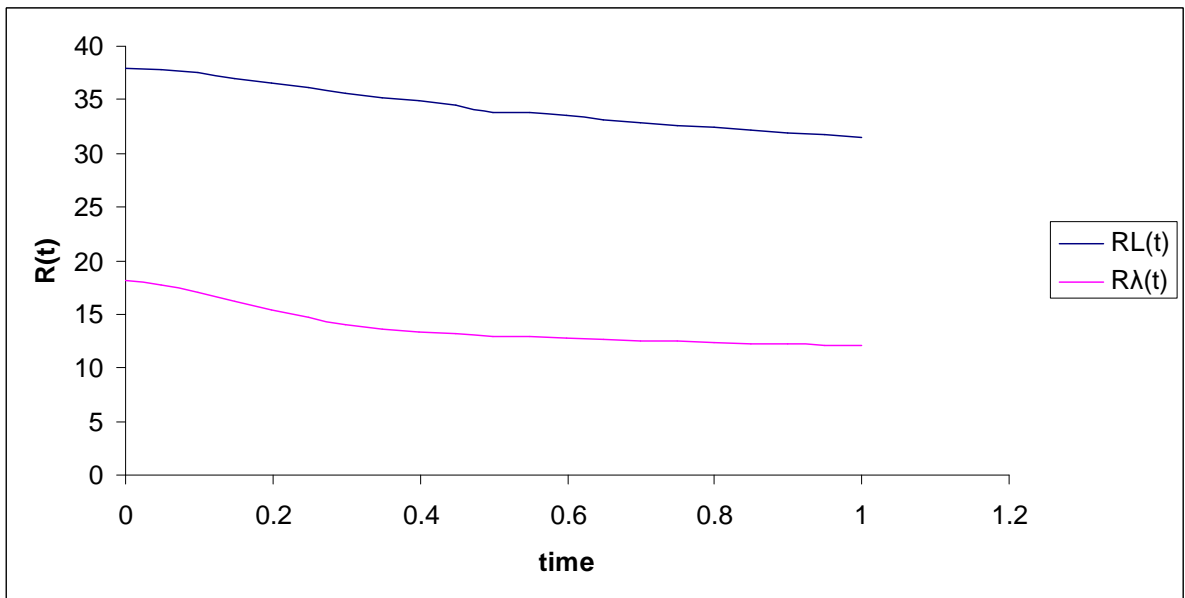


Figure 3.13 Temporal evolution of Reynolds number for spectrum II.

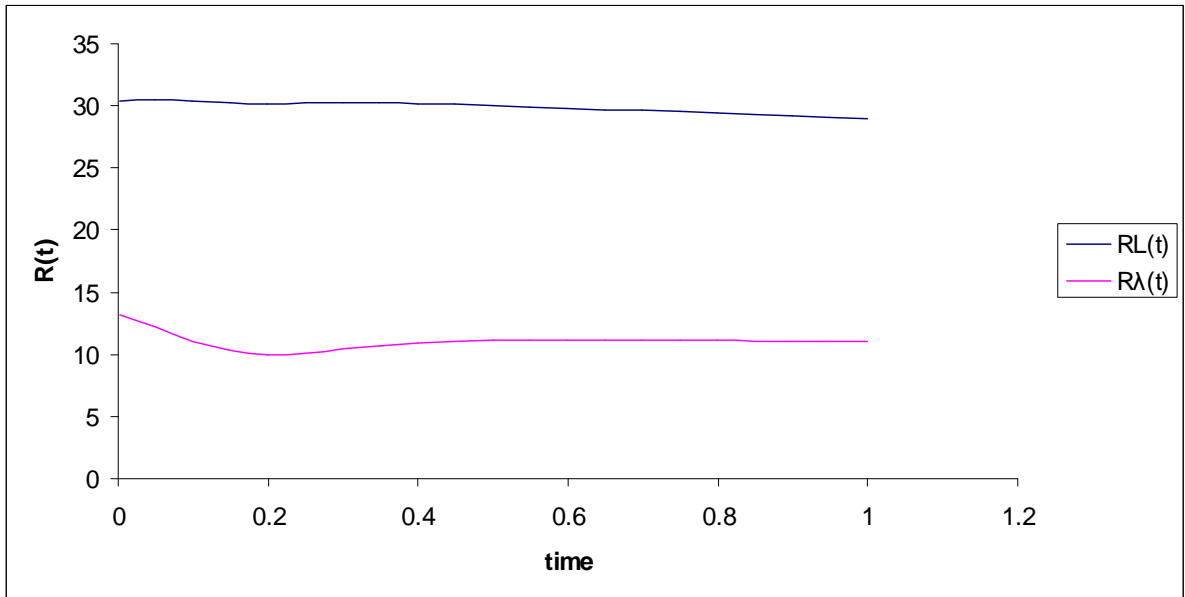


Figure 3.14 Temporal evolution of Reynolds number for spectrum III.

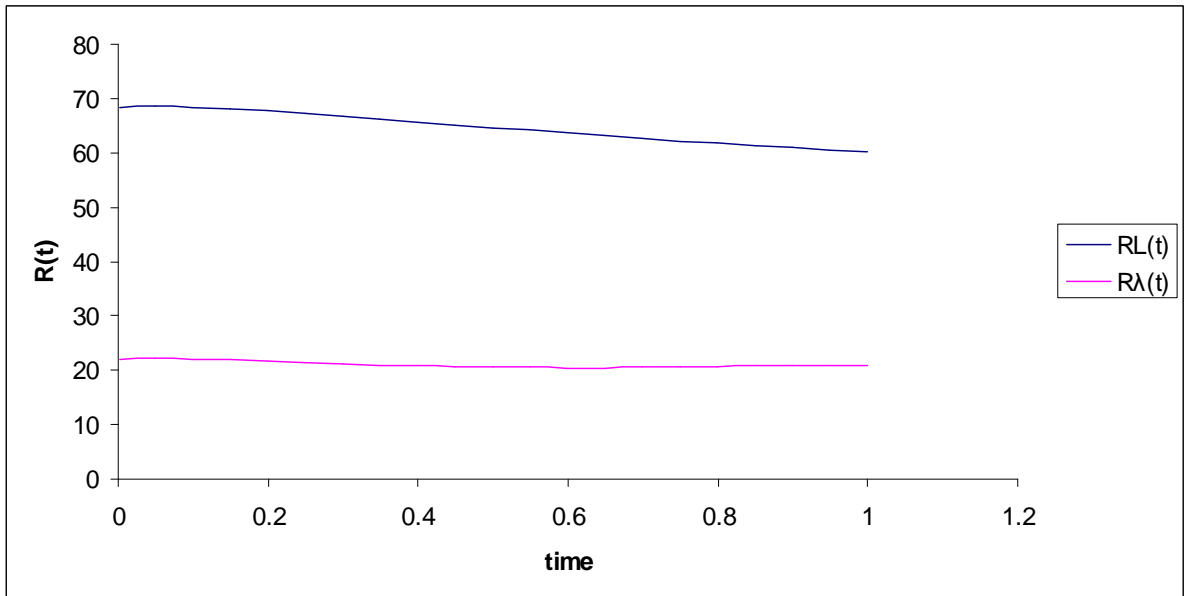


Figure 3.15 Temporal evolution of Reynolds number for spectrum IV.

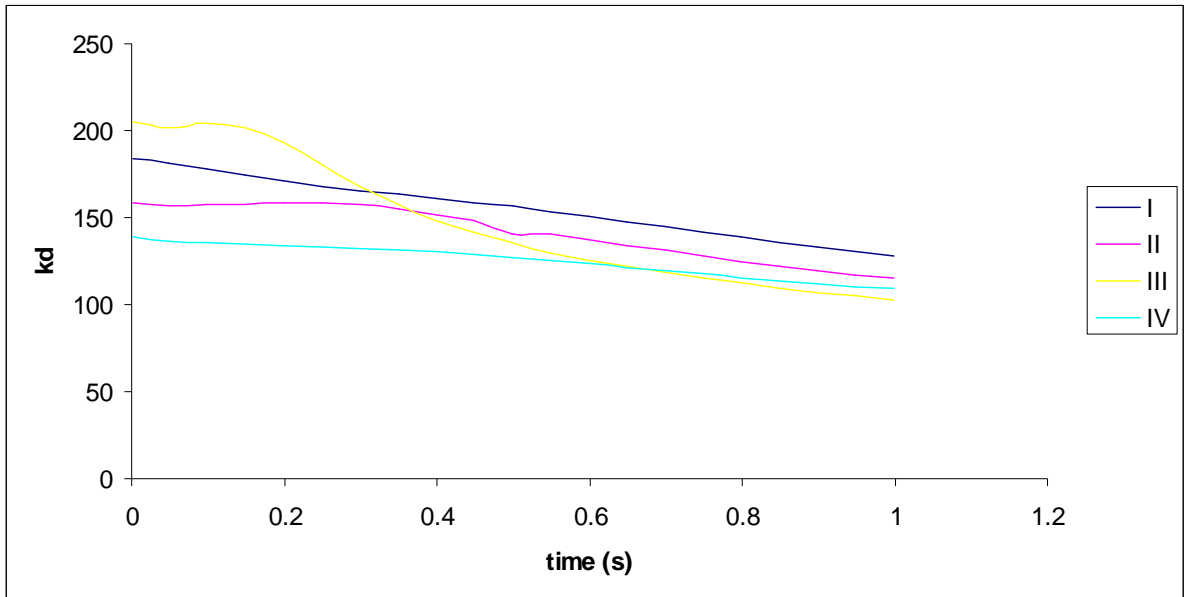


Figure 3.16 Temporal evolution of Kraichnan's characteristic wavenumber.

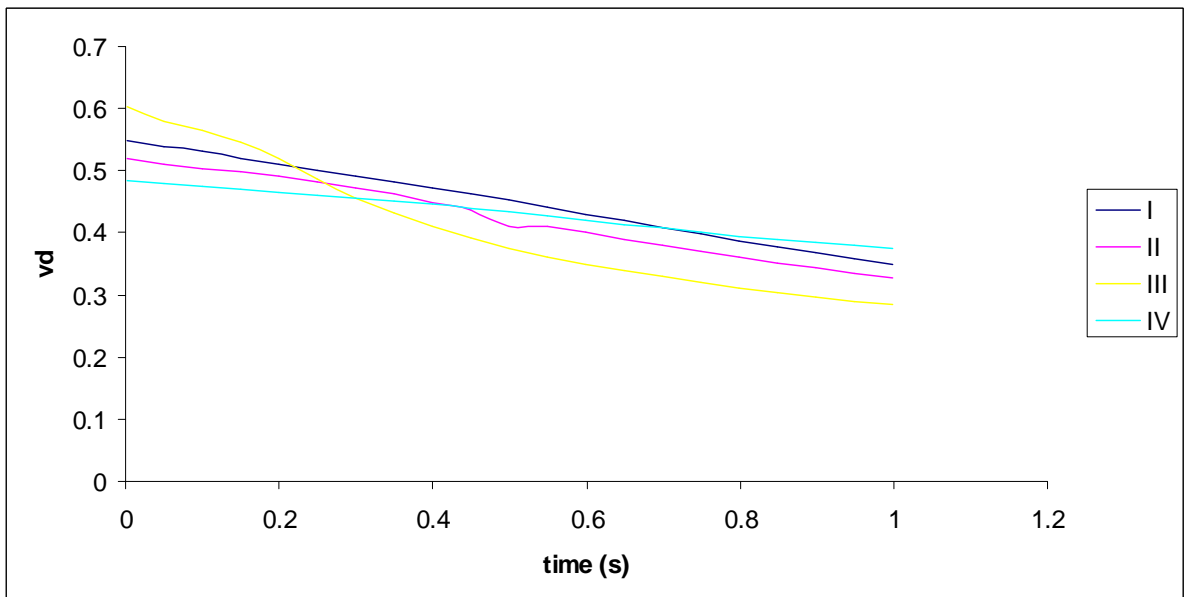


Figure 3.17 Temporal evolution of Kraichnan's characteristic velocity.

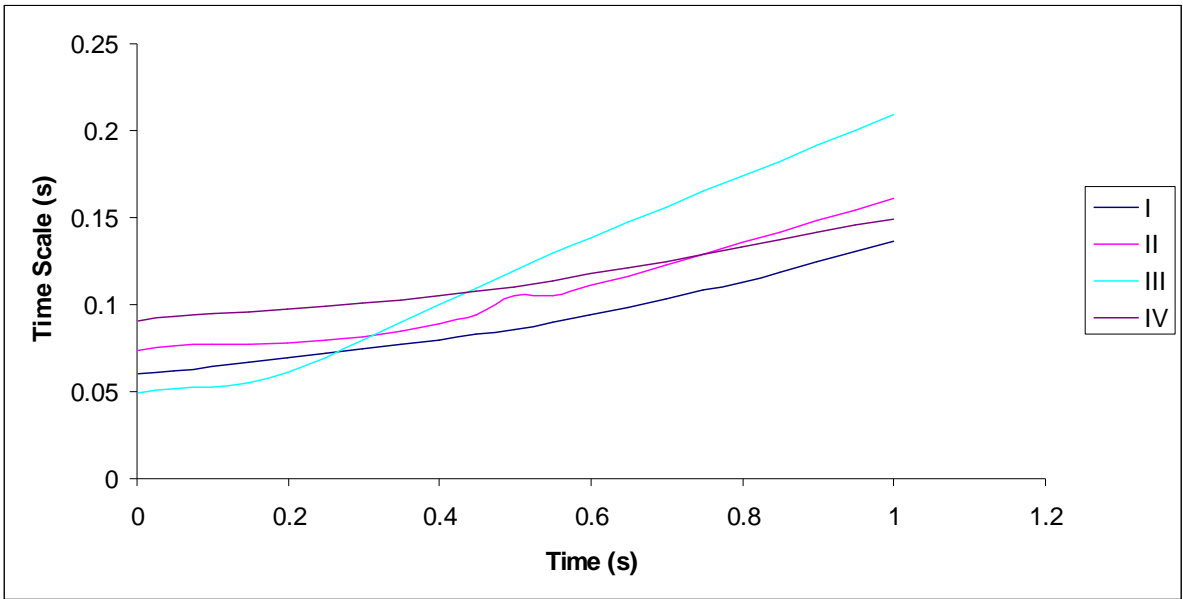


Figure 3.18 Temporal evolution of Kolmogorov time scale spectrum I, II, III and IV.

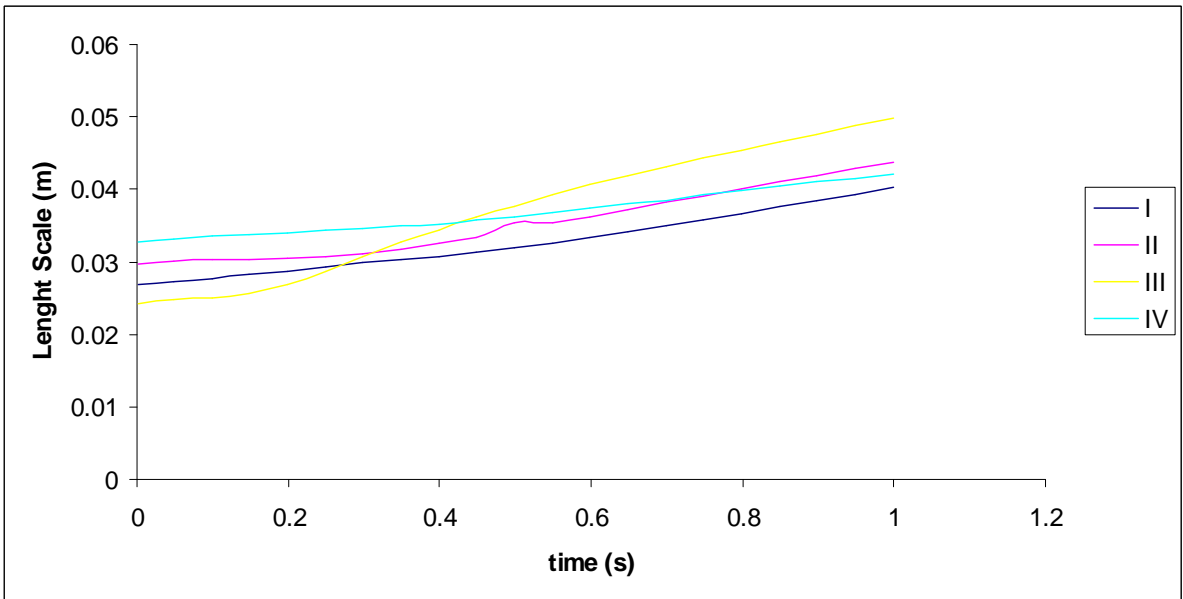


Figure 3.19 Temporal evolution of Kolmogorov length scale spectrum I, II, III and IV.

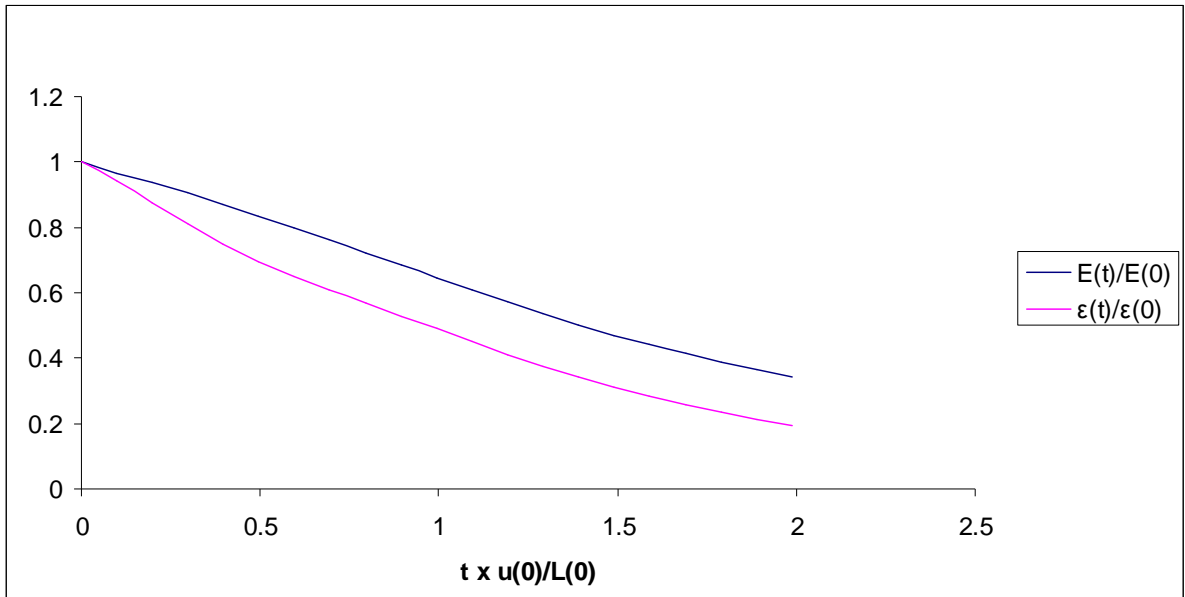


Figure 3.20 Evolution of dimensionless kinetic energy and dissipation vs. dimensionless time for spectrum I.

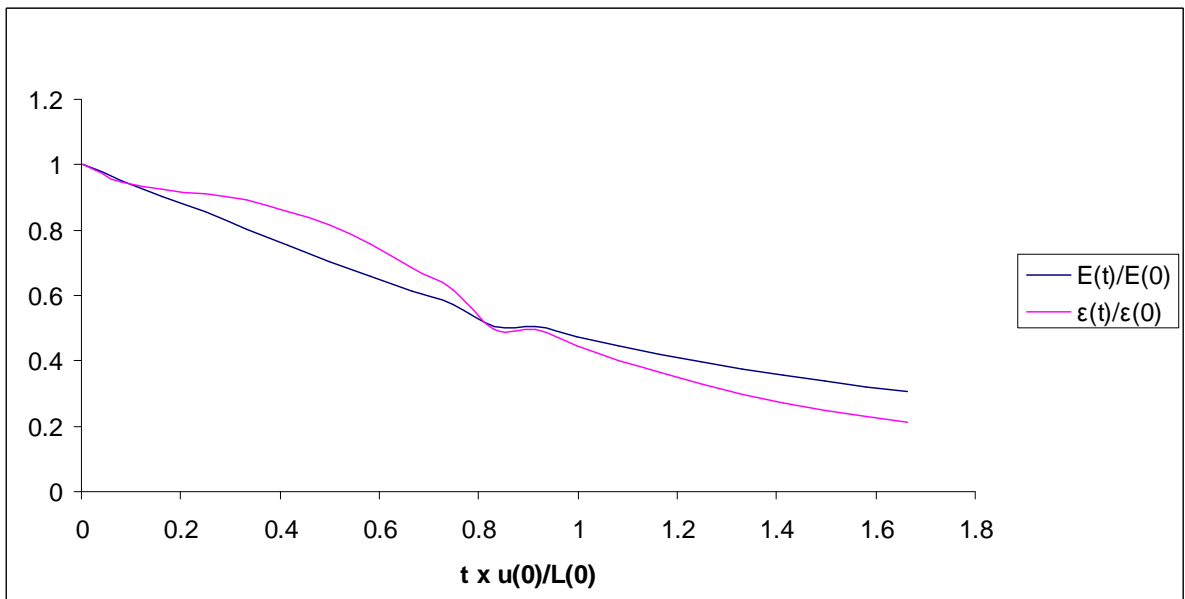


Figure 3.21 Evolution of dimensionless kinetic energy and dissipation vs. dimensionless time for spectrum II

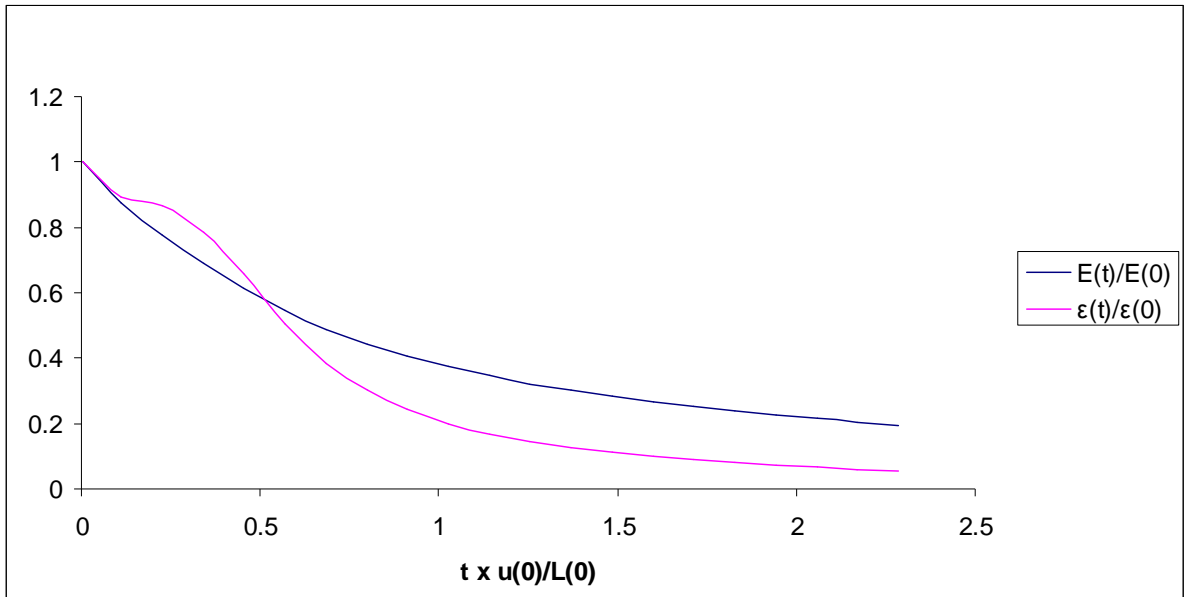


Figure 3.22 Evolution of dimensionless kinetic energy and dissipation vs. dimensionless time for spectrum III.

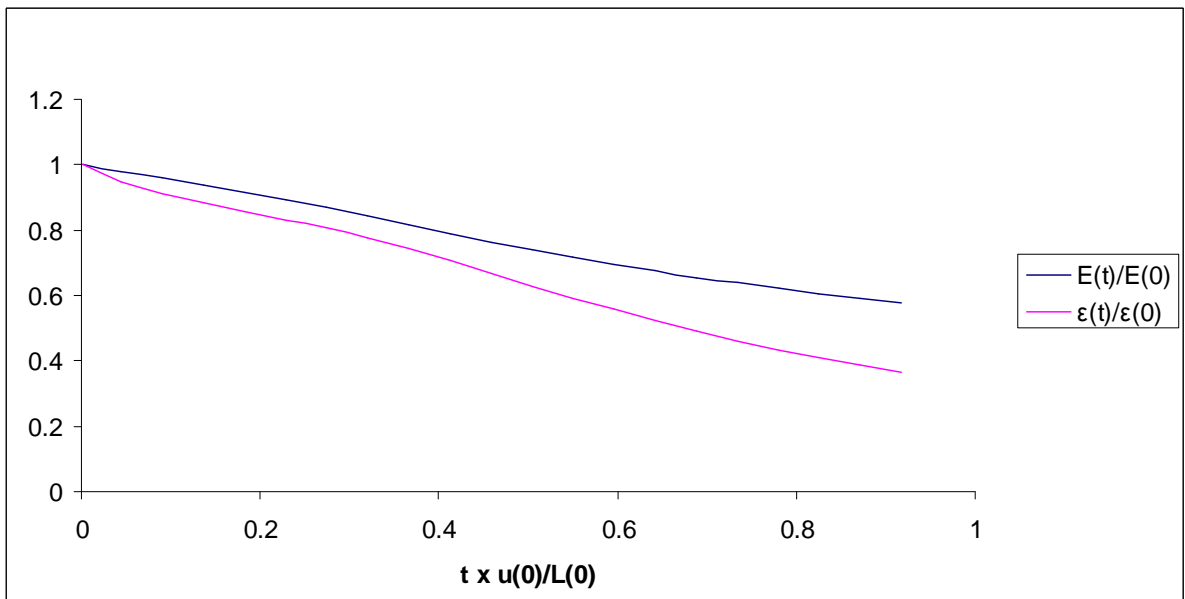


Figure 3.23 Evolution of dimensionless kinetic energy and dissipation vs. dimensionless time for spectrum IV.

4 CONCLUDING REMARKS

For this thesis work, numerical simulations of homogeneous isotropic turbulence were considered. The isotropic turbulence was simulated by numerically solving Navier-Stokes equations in Fourier wave vector and time domain by using well established numerical scheme. For the simulation purpose, four different kinds of initial energy spectra were considered. Using these spectra and method of Rogallo, initial velocity fields in wave vector domain were generated which were compatible with the spectra. The numerical simulations were then performed with these initial conditions and results were tested for convergence by performing simulation runs for different values of time steps. The temporal evolutions of four different initial spectra were calculated. From these temporal evolutions data, integral properties of isotropic turbulence were calculated and their time evolutions were presented. The information on temporal evolution of energy spectra and integral properties can be utilized for assessing various statistical theories of turbulence. In particular these data will be used to assess one such theory, namely, Variant of Local Energy Transfer theory proposed by Pandya. Also, this well tested computer program for simulating homogeneous isotropic turbulence will be enhanced, by adding inserting numerical analysis for particle tracking, for its use to study fundamental aspects of particle/droplet-laden turbulence in near future.

REFERENCES

S. W. Coppen (1998), Particle behavior using direct numerical simulations of isotropic turbulence, MS thesis, Mechanical Engineering, Tufts University.

D. A. Donzis, K. R. Sreenivasan and P. K. Yeung (2005), Scalar dissipation rate and dissipative anomaly in isotropic turbulence, *J. Fluid Mech.* **532**, pp.199-216.

R. H. Kraichnan (1959), The structure of isotropic turbulence at very high Reynolds number, *J. Fluid Mech.* **5**, 497-543.

R. H. Kraichnan (1964), Decay of isotropic turbulence in the direct-interaction approximation, *Physics of Fluids*, **7**, 1030.

A. K. Kuczaj, B. J. Geurts and W. D. McComb (2006), Nonlocal modulation of the energy cascade in broadband-forced turbulence, *Physical Review E*, **74** (1), 016306.

F. Mashayek and R. V. R. Pandya (2003), Analytical description of particle/droplet-laden turbulent flows, *Progress in Energy and Combustion Science*, **29**, pp. 329-378.

W. D. McComb (1992), *Physics of Fluid Turbulence*, Oxford University Press.

W. D. McComb and A. P. Quinn (2003), Two-point, two-time closures applied to forced isotropic turbulence, *Physica A*, **317**, pp. 487-508.

W.D. Mc Comb and V. Shanmugasundaram (1984), Numerical calculation of decaying Isotropic Turbulence using the LET Theory, *J. Fluid Mech*, **143**, pp. 95-123.

S. A. Orszag and G. S. Patterson, Jr. (1972), Numerical simulation of three-dimensional homogeneous isotropic turbulence, *Physical Review Letters*, **28**, pp. 76-79.

R. V. R. Pandya (2004), Simplification of local energy transfer theory of incompressible, isotropic, nonstationary turbulence, *Physical Review E*, **70** (6), 066307.

S. Sundaram S and L. R. Collins (1997), Collision statistics in an isotropic particle-laden turbulent suspension. Part 1. Direct numerical simulations, *J. Fluid Mech.* **335**, pp. 75-109.

R. S. Rogallo (1981), 81315 NASA TM-81315, Numerical experiments in homogeneous turbulence.

P. K. Yeung (2001), Lagrangian characteristics of turbulence and scalar transport in direct numerical simulations , J. Fluid Mech. **427**, pp. 241-274.

APPENDIX A.

Post Processing for other Values of Δt for Spectrum Evolutions

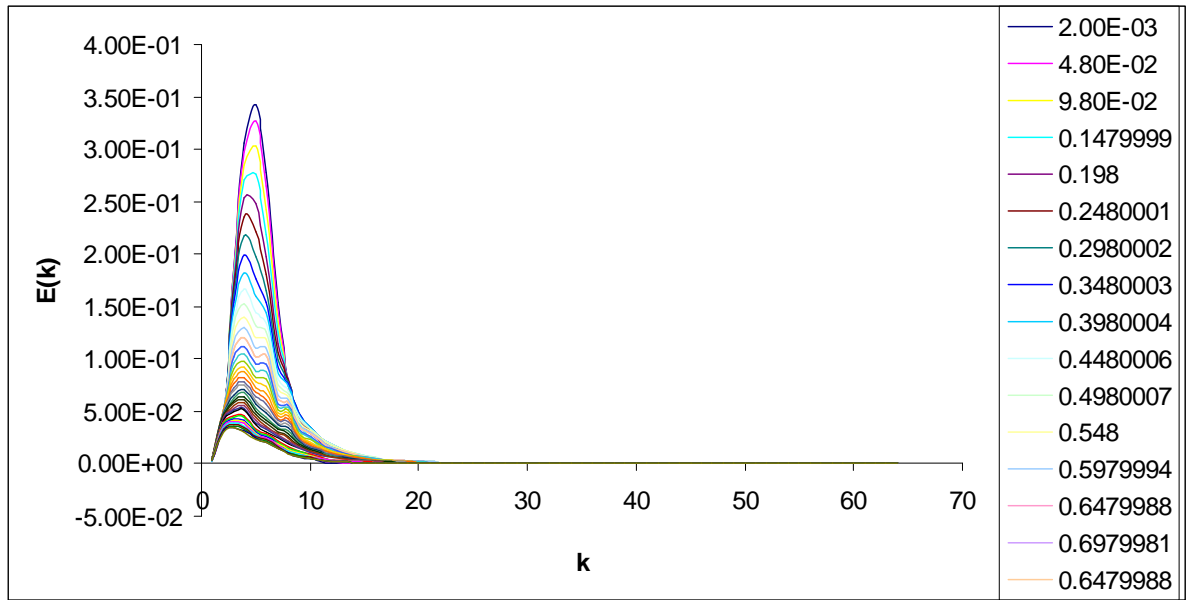


Figure 5.1 Temporal evolution of energy spectrum I for $\Delta t = 0.002$

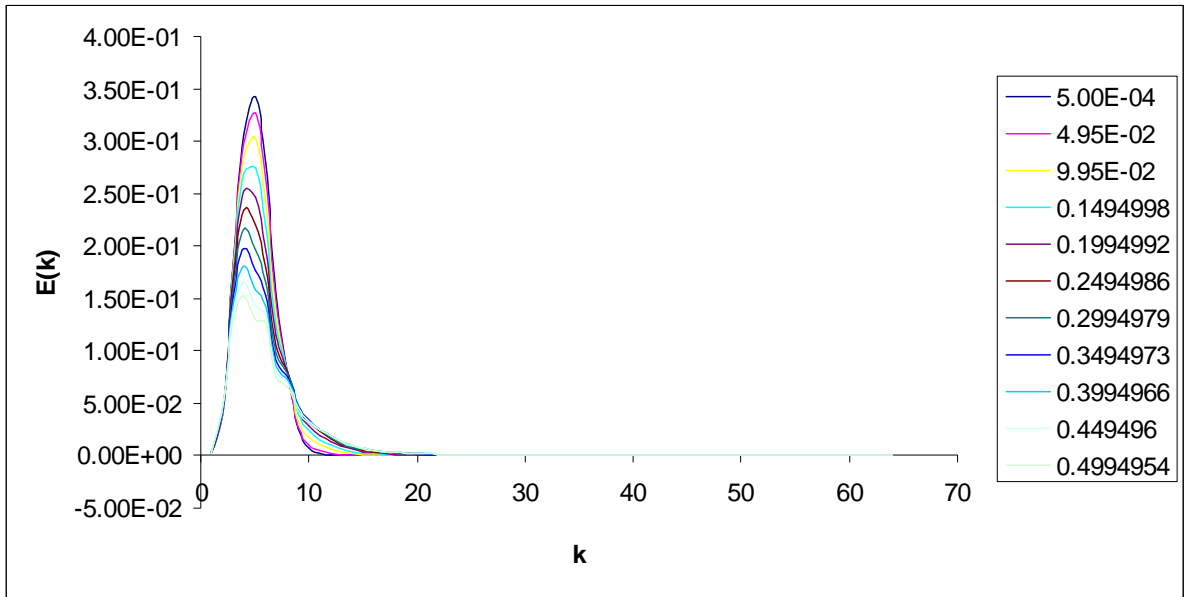


Figure 5.2 Temporal evolution of energy spectrum I for $\Delta t = 0.0005$

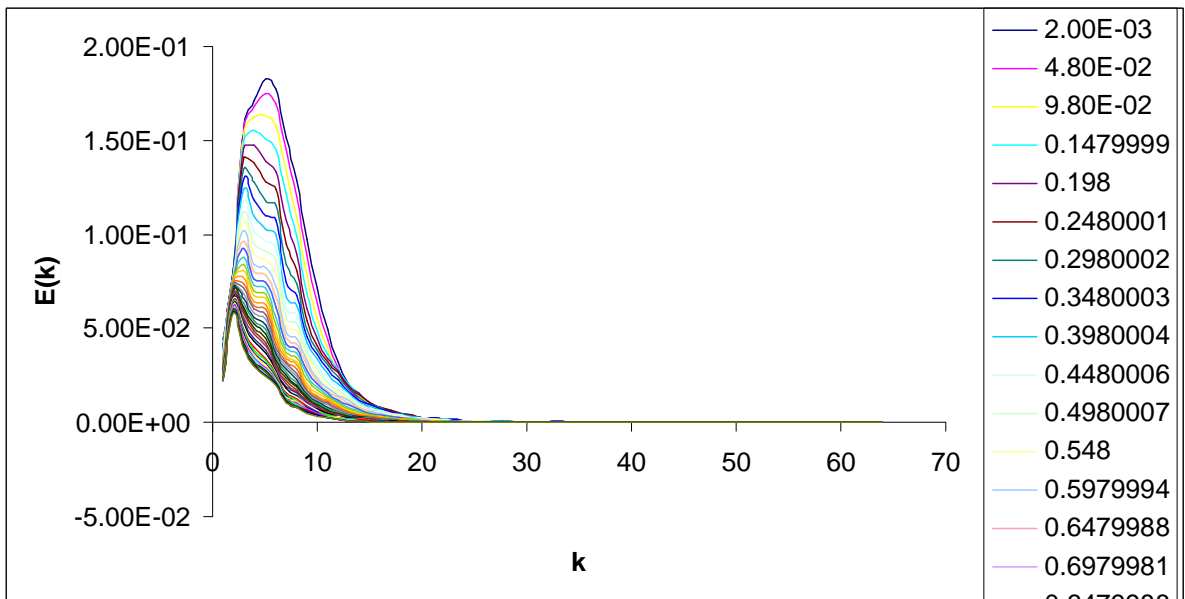


Figure 5.3 Temporal evolution of energy spectrum II for $\Delta t = 0.002$

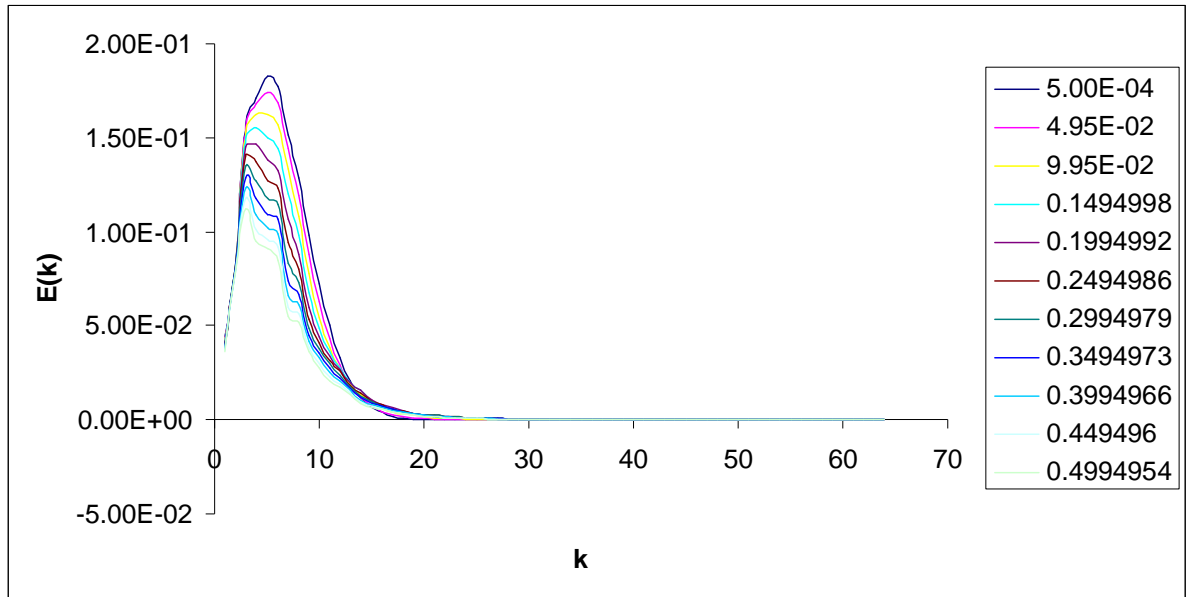


Figure 5.5 Temporal evolution of energy spectrum II for $\Delta t = 0.0005$

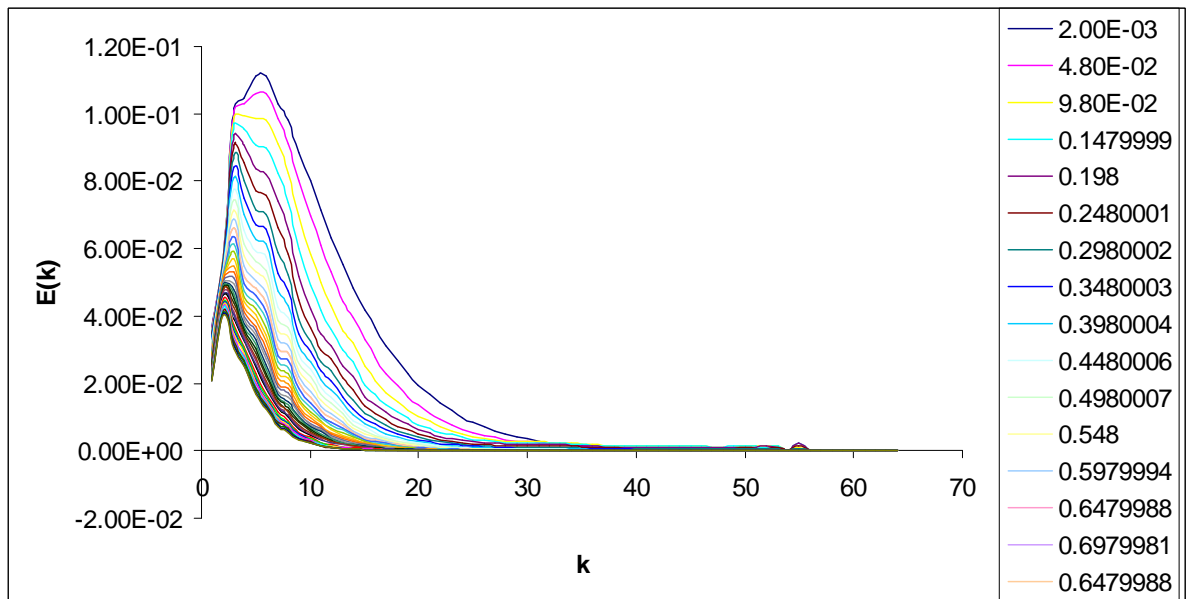


Figure 5.6 Temporal evolution of energy spectrum III for $\Delta t = 0.002$

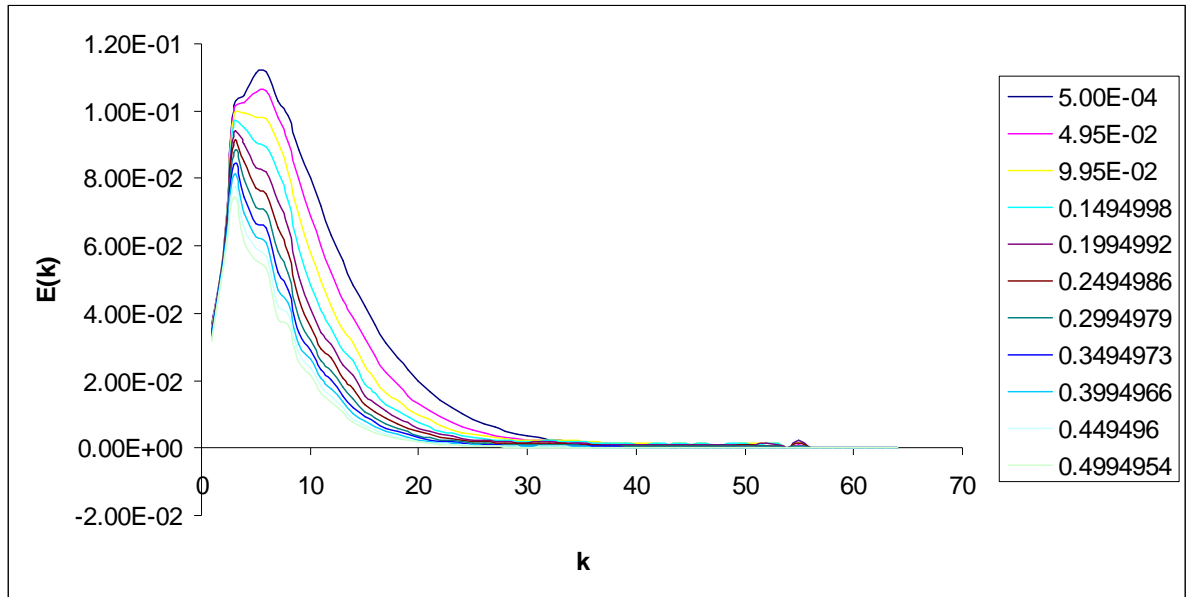


Figure 5.7 Temporal evolution of energy spectrum III for $\Delta t = 0.0005$

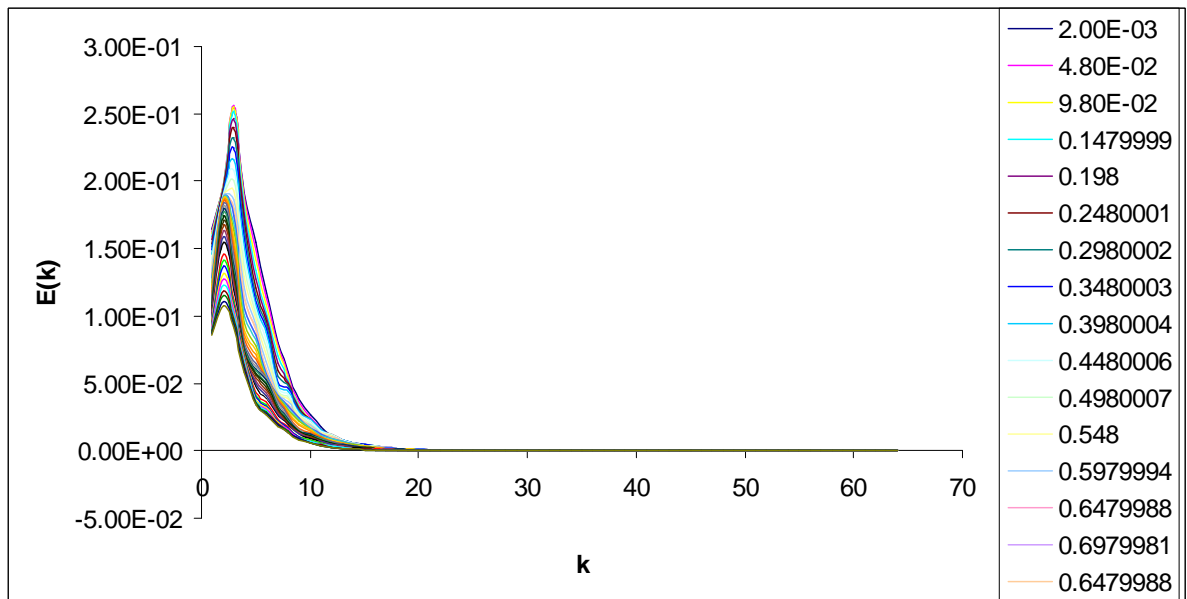


Figure 5.8 Temporal evolution of energy spectrum IV for $\Delta t = 0.002$

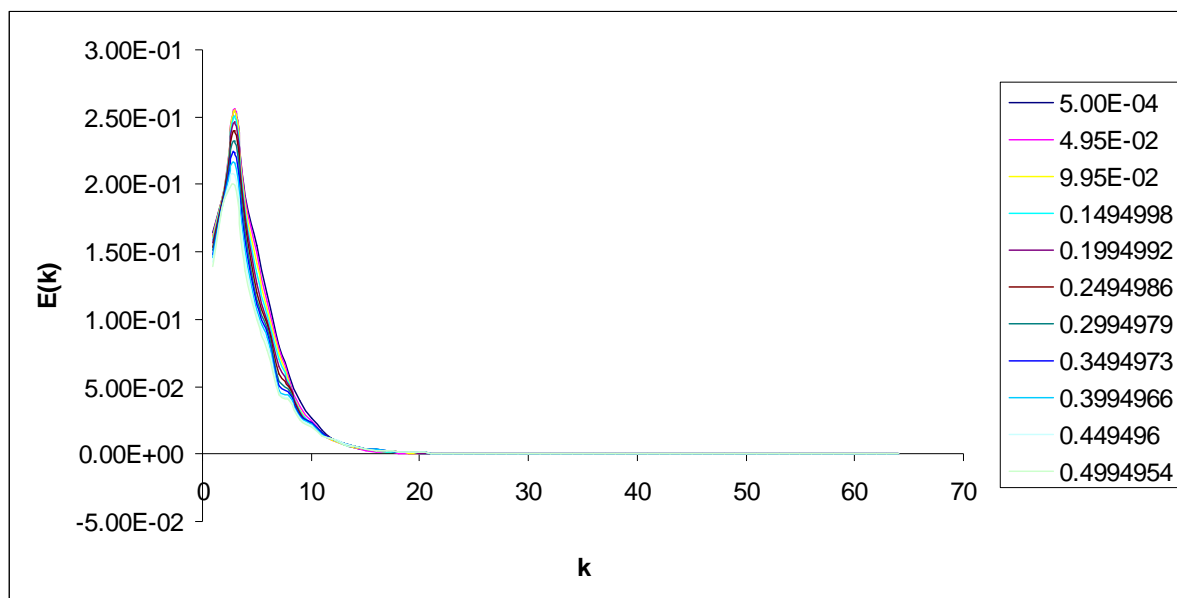


Figure 5.9 Temporal evolution of energy Spectrum IV for $\Delta t = 0.000$